A Comparative Study on VAWT Blades' Lap-Joint Designs: An Ansys Finite Element Analysis Approach

By

Harshkumar Girishbhai Patel

Thesis
Submitted to Flinders University
for the degree of

Master of Engineering (Mechanical)

Flinders University
16/10/2023

TABLE OF CONTENTS

ABSTRACT

The original and optimised designs of the blade lap joints on Vertical Axis Wind Turbines (VAWTs) are thoroughly compared in this study using Finite Element Analysis (FEA) in ANSYS. The blade lap joint, a critical structural element under considerable operational stress, is the subject of the current study. The blades benefit from increased shear resistance and tensile strength due to the use of Epoxy Carbon Woven (230 GPa) and a fibre orientation of -45, 0, 45, 0, -45 degrees. The mechanical properties of the composite material are optimised in this configuration, resulting in a longer blade lifespan. The FEA analysis revealed weaknesses in the initial design, which were resolved in an updated version. The improved design showed less stress and relocated the location of the stress from the lap edges to the z-section beam. The optimised design's safer profile was also suggested by the Tsai-Wu failure criterion, suggesting longer VAWT blade lifespans and reliable performance. In essence, this work emphasises the significance of design optimisation in renewable energy infrastructure, highlighting the integration of cutting-edge FEA technologies and material science to boost wind energy systems' efficiency and durability.

Keywords: Ansys, Lap Joint, Finite Element Analysis (FEA), Epoxy Carbon Woven, Vertical Axis Wind Turbine (VAWT).

DECLARATION

I certify that this thesis:

1. does not incorporate without acknowledgment any material previously submitted for a degree or diploma in any university
2. and the research within will not be submitted for any other future degree or diploma without the permission of Flinders University; and
3. to the best of my knowledge and belief, does not contain any material previously published or written by another person except where due reference is made in the text.

Signature of student:

Print name of student: Harshkumar Girishbhai Patel

Date: 16/10/2023

I certify that I have read this thesis. In my opinion, it is/is not (please circle) fully adequate, in scope and in quality, as a thesis for the degree of Master of Engineering (Mechanical). Furthermore, I confirm that I have provided feedback on this thesis and the student has implemented it minimally/partially/fully (please circle).

[redacted]

Signature of Principal Supervisor:

Print name of Principal Supervisor: Amir Zanj

Date: 16/10/2023

ACKNOWLEDGEMENTS

First and foremost, I would like to convey my deep appreciation to my supervisor, Amir Zanj, for his excellent direction, unwavering assistance, and mentorship throughout my thesis. His profound knowledge and perceptive observations have provided important guidance for this thesis.

Special thanks to my classmate Nitesh Poudel, for his substantial contribution to the creation of the CAD models. His thesis, titled "Design Automation of Manufacturing Process for VAWT Blade and its Mould by Parametrization," supervised by Amir Zanj, has been highly influential and has laid strong groundwork for my research.

Special thanks to my other classmate Deepak Sapkota, who has played a crucial role in the validation process. The contribution of his research on "Design, Development, and Strain Measurement System for VAWT Blades" has played an important role in guaranteeing the precision and dependability of my results.

I would also like to express my appreciation to Flinders University's Tonsley campus for granting me access to the laboratory model of a VAWT blade. This reduced-scale variant of the Darrieus VAWT has proven to be an indispensable asset for my study. Also, special thanks to VAWT-X Energy, the pioneering startup located in South Australia, for their development of this concept and their valuable contribution to the progress of renewable energy solutions.

Finally, I would like to thank everyone who has indirectly helped my study and provided their support throughout this endeavour. The support and confidence you have shown in my skills have been the primary motivators for my persistence and commitment.

LIST OF FIGURES

LIST OF TABLES

INTRODUCTION

The emphasis on utilising wind energy has significantly increased as the global energy landscape undergoes a seismic shift towards sustainable and eco-friendly alternatives. An iconic symbol of this transition, wind turbines stand tall and strong, harnessing the kinetic energy of the wind and transforming it into useful electrical power. A possible alternative to the more traditional Horizontal Axis Wind Turbines (HAWTs) is slowly developing among the numerous wind turbine designs called Vertical Axis Wind Turbines (VAWTs). The importance and promise of VAWTs as the world moves into the era of renewable energy cannot be overstated. Their unique advantage comes from their natural ability to collect wind from every direction. Unlike their horizontal axis rivals, VAWTs can capture wind energy regardless of the direction of the wind's flow. This not only improves the effectiveness of electricity generation but also makes the system more adaptable, especially in areas with changeable wind patterns. (ARCADIA, 2017).

Every invention, nevertheless, comes with a unique set of difficulties. The distinctive operational dynamics of VAWTs, particularly about the blade designs, raise particular structural difficulties. While a blade may appear to be one solid piece, it is actually made up of several intricate parts that affect its durability, strength, and aerodynamics. The lap joint is one of these essential components. A lap joint may first appear to be nothing more than the simple overlapping of two parts, but in truth, it is essential to maintaining the blade's structural integrity. A damaged lap joint can seriously limit a VAWT's effectiveness and longevity, possibly resulting in catastrophic failures or a shorter operating life.

Figure 1: Laboratory model of a Vertical Axis Wind Turbine

(source: Flinders University)

This study involves the analysis of a laboratory model of a Vertical Axis Wind Turbine (VAWT) blade located at Flinders University's Tonsley campus which is shown in Figure 1. This specific model is a scaled-down version of the Darrieus VAWT which is presented in Figure 2, which belongs to VAWT-X Energy, a developing start-up with headquarters in South Australia that is committed to the certification and marketing of its patented 2-bladed air-foil technology for extensive manufacturing. (Vawt-X Energy, n.d.). The Darrieus VAWT has a hub height of 5.0 metres and a rotor diameter of 3.4 metres. In comparison, the laboratory prototype located at Tonsley has a hub height of 1 metre and a rotor diameter of 0.682 metres.

Figure 2: Vertical Axis Wind Turbine at Vawt-X

(Source: Vawt-X Energy, n.d.)

In this research, the Ansys 2022 Version was used to do a Finite Element Analysis (FEA) on an assembly of 11 blades for both the original and optimised blades with the trimmed end section similar to the laboratory model's blade structure. Figure 3 and Figure 4 present the original VAWT blades' lap joint and the final optimised blades' lap joint design correspondingly. (All the other optimised designs before reaching to final optimised one, are presented in the appendices section of this thesis.)

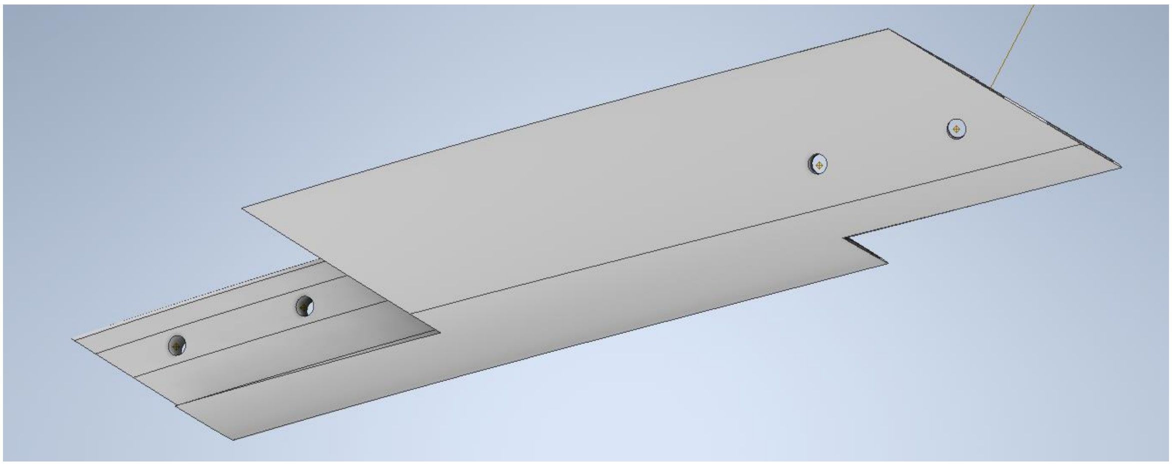

Figure 3: CAD Model of Original VAWT Blade

(Source: Design Automation of Manufacturing process for VAWT Blade & its Mould by Parametrization by Nitesh Poudel)

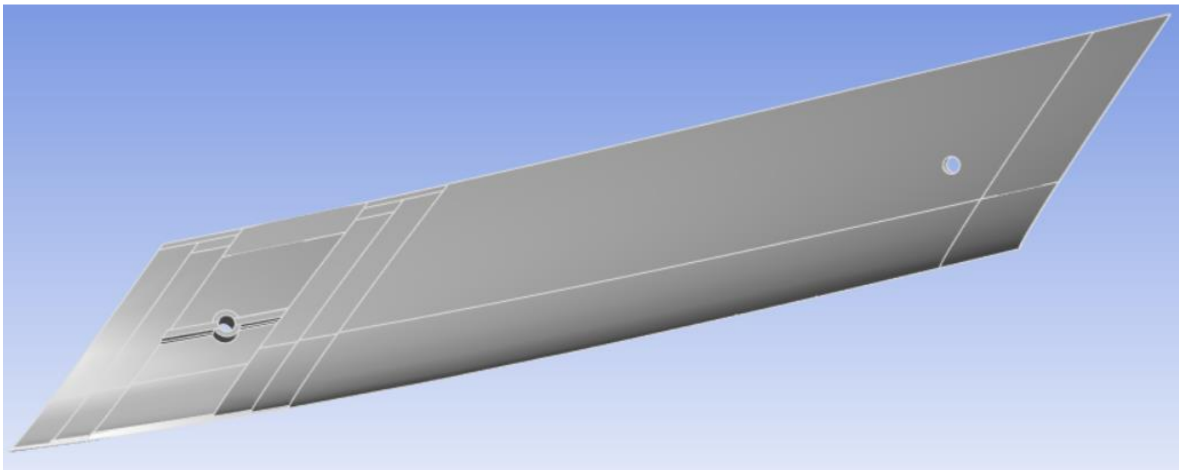

Figure 4:CAD Model of Optimised VAWT Blade

(Source: Design Automation of Manufacturing process for VAWT Blade & its Mould by Parametrization by Nitesh Poudel)

AIMS

- **Analysis of Current Design's Performance:** To assess and evaluate the performance of the current blades' lap-joint design under various simulated operational circumstances.
- **Selection of Materials**: To research and compare several materials for the lap joint, evaluating their mechanical properties, durability, and compatibility for VAWT blade applications.
- **FEA Using Ansys:** To utilise the excellent capabilities of Ansys for finite element analysis, enabling the simulation of various stress, strain, and performance scenarios of the lap joint designs.
- **Comparison of Various Design Alternatives:** Based on the FEA results, compare a variety of lap-joint designs, taking into consideration elements like stress distribution and overall structural integrity.
- **Optimisation and Selection:** Based on extensive research, determine and choose the best-optimised lap-joint design that exhibits greater performance, durability, and resilience.

LITERATURE

Previous studies on lap joint

Bonded lap joints are of significant importance in the optimisation and enhancement of the performance of structures made from carbon fibre-reinforced polymer (CFRP) materials. According to Kupski and De Freitas (2021), it has been emphasised that conventional joint configurations, particularly single overlap joints, frequently give rise to elevated peel stresses. This can lead to abrupt failure and decreased strength when these joints are combined with metal equivalents. The aforementioned limitation hinders the overall effectiveness and potential of CFRP in constructions where these joints are essential. The authors provide insights into the importance of joint design in enhancing lap shear strength and highlight the difficulty associated with delamination failure, a commonly seen kind of failure in composite bonded joints. The prevailing methods in the industry commonly utilise quasi-isotropic carbon fibre reinforced polymer (CFRP) layups owing to their convenient manufacturing process; however, they may exhibit inefficiencies under certain stress circumstances, particularly in bonded joints. Kupski and De Freitas (2021) provided a comprehensive analysis of many aspects that have the potential to impact the strength of joints. These factors encompass long-standing areas of investigation, such as the influence of overlap length and adhesive thickness, as well as more recent developments like functionally graded adhesives. One significant conclusion drawn from their thorough examination is the significant potential that exists in enhancing the out-of-plane qualities associated with certain parameters of laminates, such as fibre orientation, ply thickness, and ply interleaving. The study offers a road map by emphasising new approaches and the difficulties they entail, as well as the huge untapped potential of CFRP-bonded joints, pointing towards a future replete with cutting-edge joint designs.

Chen, Wang, and Huang (2019) examined the effects of nonflat surfaces on joint performance in their study of the structural integrity of adhesively bonded joints. Their in-depth analysis showed that altering the shape of the bonded area, especially through embedded reinforcements, significantly increased the strength of such joints. Their study explores how changing the geometric design of adhesively bonded joints can increase their strength. The performance of these joints under nonflat interfaces is carefully assessed in their study using both computational and experimental techniques. Important discoveries include the identification of a distinct two-stage failure process and the two main variables affecting joint strength. Surprisingly, after optimisation, the nonflat-interface specimens performed 45% better under ultimate load and 52% better under average shear stress than their flat-interface counterparts. Furthermore, these improved joints maintained their load-bearing capacity even when paired with deliberate flaws, losing weight without the need for an additional mould. These developments could completely alter how bonded joints are used in industry. In relation to this thesis, Chen et al. (2019) provide insightful information on design optimisation considerations, specifically the benefits of nonflat joint surfaces for improving the strength and performance of bonded joints.

According to the research of Lindkvist and Nicolausson (2019), the vertical beam in wind turbine blades gives considerable structural benefits. The VAWT blade design has numerous structural parts, in contrast to traditional wind turbine blades, which are created as a single cohesive unit. The vertical bars, also known as Z-section beams in the wind turbine context, are among these parts and are vital in preserving the spatial separation between the horizontal beams. This guarantees the stability and structural integrity of the whole truss system. These vertical bars primarily support compressive pressures that stabilise the horizontal beams and keep them from collapsing inward, especially in the presence of wind loads. The total effectiveness and endurance of wind turbine blades are improved by this ground-breaking design, which emphasises the function of the vertical beams and makes them more resistant to variable wind conditions. Hence, by taking inspiration from the research of Lindkvist and Nicolausson (2019), the vertical beam is utilised in the z section of the optimised design of the VAWT blades' lap joint design.

Composite Material Selection

Wind power has emerged as a promising solution in the quest for technical advancements that might lead to more efficient energy results. With the fast shift in the energy sector, there is an increasing need to improve the efficiency and longevity of wind turbines. The necessity for an in-depth understanding of wind turbine behaviour in different loading conditions is evident. The performance of four various composite materials was thoroughly studied in research done by Gukendran et al. (2023). Their research utilised ANSYS Workbench software to conduct an in-depth examination of a typical wind turbine blade. The composite materials were subjected to several tests to evaluate metrics such as total deformation, equivalent Von-Mises stress, maximum shear stress, and strain energy. The obtained data was thoroughly recorded. The use of composite materials in wind turbine blades has become more prevalent due to their advantageous lightweight properties, resulting in improved strength and efficiency for power generation. Various materials, such as epoxy, Aramid fibres, and Carbon Fibre Reinforced Polymer (CFRP), were compared. The fundamental aspect of composite materials is the seamless integration of a minimum of two distinct materials, leading to enhanced qualities that surpass those of the separate components. When compared to other composite materials, epoxy carbon exhibits minimum deformation and excellent stress properties, suggesting its better resilience and durability. Epoxy carbon, known for its carbon fibre composition, has gained prominence as a leading material because of its notable characteristics, such as significant tensile strength, low weight, excellent chemical resistance, and outstanding ability to withstand high temperatures. The comprehensive study undertaken by Gukendran et al. (2023) provides substantial evidence supporting the justification for choosing epoxy carbon fibre as the key material for this thesis.

The research conducted by Boudounit et al. (2023) represents a significant contribution to the field of composite material arrangements. In their study, the authors made the deliberate choice to utilise a seven-ply structure, with each individual ply measuring 0.94 mm in thickness, which can be seen in Figure 5. The underlying justification for this configuration is the equitable allocation of fibres to endure forces from several directions and to reduce any possible warping resulting from mechanical or thermal factors. The researchers conducted an extensive study that demonstrated the significant importance of layer orientation in affecting the overall mechanical performance of the composite material, particularly when subjected to complicated loading conditions commonly encountered in real-world applications.

Figure removed due to copyright restriction.

Figure 5: Fibre Orientation

(source: Boudounit, H., Tarfaoui, M. and Saifaoui, D., 2023)

The author has utilised the orientation of the fibres, shown by the sequence of angles 45, 0, -45, 0, 45, 0, -45 degrees. The aforementioned configuration is presented in Figure 5 and has been experimentally proven to yield an ideal and effective mechanical response, effectively bringing together axial stiffness with biaxial resilience. The layers oriented at 0 degrees are designed to withstand the principal loading direction, thereby contributing to the overall strength of the VAWT blade. On the other hand, the alternating orientations of -45 and 45 degrees serve to strengthen the blade's ability to resist shear stresses and promote a balanced distribution of forces. In addition, the implementation of a symmetrical sequence in the construction of the laminate serves to establish a state of equilibrium, reducing the likelihood of warping or distortion arising from residual tensions or temperature influences. Hence, the approach employed for fibre orientation in this thesis is based on the findings of Boudounit et al. (2023) but has been adapted to accommodate the specific manufacturing limitations and goals of the current research.

FEA Analysis

Yeh and Wang (2017) conducted an in-depth study on the stress distribution and deformation of a 5 MW wind turbine blade. The in-depth investigation of the composite wind turbine blade, which consists of a sandwich structure consisting of outer carbon fibre cloth/epoxy composites, inner glass fibre layers, and a PVC foam core, revealed significant insights into the structural response of the blade when subjected to different stress conditions and loads. The stress distribution and deformation of the blade were evaluated by the authors using the FEA software ANSYS. The assessment considered various pitch angles and angular positions, with a particular focus on specific stress hotspots. These hotspots were located at the junction of different airfoil sections near stiffener edges. The analysis revealed a significant correlation between the stress response of the blade and its angular position and pitch.

Yeh and Wang's (2017) research has significantly advanced the field, particularly in understanding the effects of various pitch angles and angular positions on stress distribution. Their findings have not only established a comprehensive framework for evaluating stress and deformation in similar structures but have also stimulated further exploration into enhancing blade design to minimise stress accumulation during operation. Expanding upon the aforementioned discoveries, the present thesis shifts its focus towards a specialised investigation of stress distribution. This shift entails a departure from the previous emphasis on angular aspects to delve more profoundly into comprehending the intricate patterns of stress behaviour. The objective is to gain insights into the effects of such behaviour on the durability of blades, the integrity of structures, and overall performance, particularly when subjected to diverse operational and environmental circumstances. As a result, this gives rise to a comprehensive and refined approach that, while acknowledging the initial FEA methodology employed by Yeh and Wang (2017), establishes its unique position in enhancing the comprehension and implementation of stress analysis in the design and optimisation of wind turbine blades.

Designing wind turbines requires careful consideration of the loading conditions. Numerous loads are placed on wind turbines, and heavy loads can cause failure. These pressures include gravity loads that change direction during blade rotation, mostly generating edgewise and flapwise bending caused by aerodynamic pressure (lift and drag) on the blade. The changing of gravitational force direction in its local coordinate system also causes tension-compression cyclic loading at the blade's root, particularly at its leading and trailing edges. Centrifugal forces are still very minor because of the sluggish rotational speed of the wind turbine blades, despite the fact that this cyclic loading significantly affects the blade life. (Salimi-Majd, D., Azimzadeh, V. and Mohammadi, B., 2015). Inspired by these loading conditions, this study utilizes a scaled laboratory model with reduced values for a more controlled analysis.

The Tsai-Wu failure criterion is a widely used method for predicting failure in composite materials. In the context of design optimisation of the VAWT blades' lap joint, the use of FEA is of utmost importance. Particularly when considering the utilisation of composite materials for the construction of the blades, it becomes crucial to have an extensive knowledge of failure criteria specific to such materials. The analysis of composite materials, which exhibit anisotropic behaviour and have properties that are influenced by fibre orientation, commonly uses the Tsai-Wu failure criterion. Composite materials, especially those composed of fibre-reinforced polymers, exhibit anisotropic properties. This implies that their stiffness and strength change with direction. Therefore, while evaluating probable failure modes, it is important to consider these directional variations. The framework presented in this study offers a complete approach to predicting the initiation of failure in composite materials when exposed to challenging loading conditions. (Diniz et al., 2019).

ASSUMPTION AND LIMITATION

Assumptions

- **Temperature Neutrality:** One of the major presumptions in this study is that the effects of temperature changes are neglected. This indicates that the analyses do not take into account potential thermal loads and associated deformations that could result from temperature changes.
- **Perfect Bonding:** For the bonded lap joint of the laboratory model blades that are attached using glue, the assumption of perfect bonding is made. This assumes that the interface between the bonding surfaces is free of small gaps or the possibility of debonding.
- **Simplified Aerodynamic Loading:** It is assumed that the aerodynamic forces pushing against the VAWT blade are simple. This can include treating the wind force as a uniform load applied to the surface of the blade, which might not adequately reflect complicated aerodynamic interactions in real-world settings.
- **Homogeneous Material qualities:** It is presumed that the volume of the Epoxy Carbon Woven material utilised in the model is homogeneous and has constant qualities. This implies that any potential flaws, faults, or changes in the material composition are not taken into account in the analysis.
- **Static Loading conditions:** The study assumes that the VAWT blades will be subjected to mostly static loading conditions. This means that analyses place more emphasis on steady-state conditions than dynamic or transient forces, which might vary rapidly over time.

Limitations

- **Vibration analysis:** Vibration-induced stresses or potential resonant frequencies are excluded from the research.
- **Software Restraints:** The Ansys 2022 version was used to carry out the FEA analysis. Despite being prominent in the field of finite element analysis, Ansys has inherent constraints in terms of processing power, simulation quality, and feature sets in each of its cycles. This can limit the scope or depth of some analyses.

- **Material Assumptions:** Although Carbon fibre's qualities are taken into account for the analyses, the precise properties of materials can change depending on the used FEA software's material data, which may cause a small amount of difference in the outcomes.
- **Scale Restrictions:** The research is based on a laboratory model, which might not accurately depict all of the difficulties and interactions that a commercial-scale blade would encounter.

METHODOLOGY

To carry out the FEA analysis in Ansys, various lap joint designs of VAWT blades went through all the steps mentioned in the flowchart named "Figure 6". At the end of the FEA analysis, results were compared, and if the results were not satisfactory, the whole process was repeated with the new optimised design. For simplicity of methodology, the final optimised design methodology is presented in the following thesis.

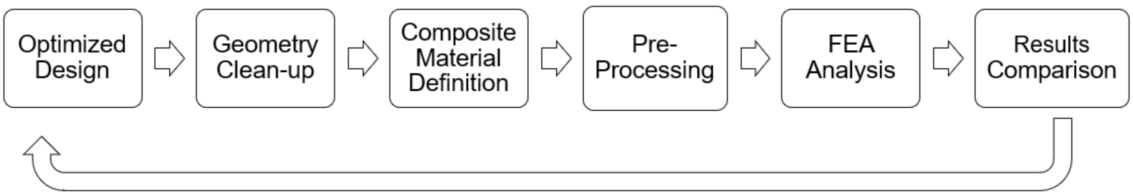

Figure 6: Flowchart Showcasing Methodology

Geometry Clean-up

The primary objective of this phase was to carefully refine the computer-aided design (CAD) geometry of an 11-blade VAWT assembly in order to make it suitable for a precise FEA. (The engineering drawing of the final optimised design is presented in the appendices section of this thesis.)

The CAD model depicting the assembly consisting of 11 blades was imported into the ANSYS SpaceClaim environment.

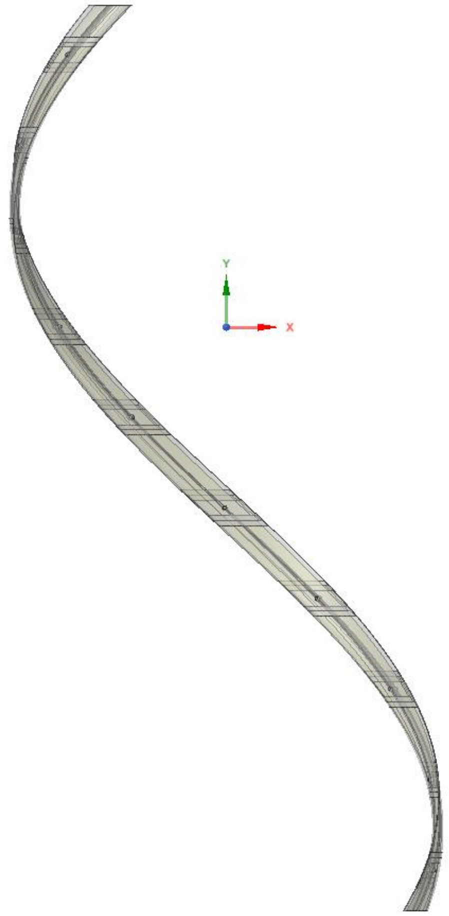

Figure 7: Optimised 11 Blades Assembly with Trimmed End Sections

To enhance computing efficiency during the FEA procedure, the 3D solid geometry was transformed into a shell representation. The conversion process was conducted using the 'Prepare' tab feature in the programme. The blade assembly was chosen in its entirety and thereafter transformed into a shell format. A shell thickness that was established by empirical means was evenly applied. The subsequent focus was directed on the endpoints of both the first and eleventh blades. By employing the 'Split' and 'Trim' functions in SpaceClaim, the blade ends were carefully eliminated, ensuring that symmetrical and precise geometric modifications were made to ensure uniformity throughout the assembly which can be seen in Figure 7.

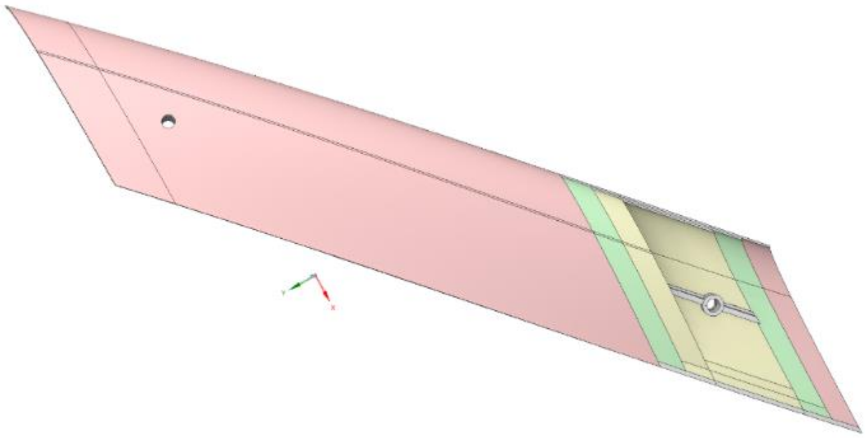

Figure 8: Optimised Blade Before Clean-Up

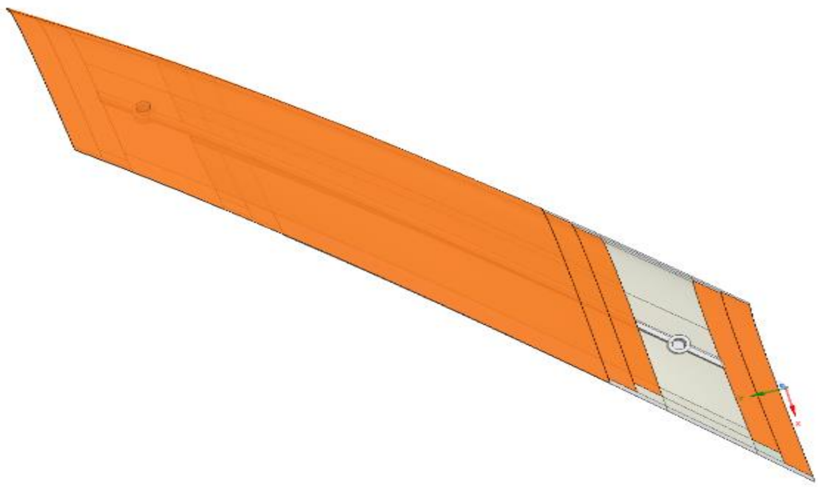

Figure 9: Optimised Blade After Clean-Up

The refinement and cleanup of the geometry are necessary steps in the process. Upon conducting a comprehensive examination of the assembly, several geometric flaws were identified, including instances of overlapping areas, unintended gaps, and overly sharp delineations, which can be seen in Figure 8. The strategic use of SpaceClaim's "Pull," "Move," "Fill," and "Combine" capabilities effectively addressed the abnormalities. Non-essential geometric elements, which may not have a significant impact on the final analysis but might present computing difficulties, were carefully removed, which can be seen in Figure 9. Considerable emphasis was placed on ensuring that the altered areas were meticulously smoothed to provide a flawless geometric appearance. The assembly underwent a thorough evaluation from several angles to guarantee its integrity and preparedness for FEA. Figure 10 shows the reduced number of faces of 938 which was before geometry clean-up was 1243.

Details of "Layered Section"	
Scope	
Scoping Method	Geometry Selection
Geometry	938 Faces
Definition	
Coordinate System	Center mass coordinate System
Offset Type	Middle
Layers	Worksheet
Suppressed	No
Material	
Nonlinear Effects	Yes
Thermal Strain Effects	Yes
Graphics Properties	
Layer To Display	All Layers
Properties	
Total Thickness	1. mm
Total Mass	0.8485 kg

Figure 10: Layer Section

Composite Material Definition

The need for optimal performance under the operational conditions of the VAWT blades and theoretical data served as the foundation for the current research's material selection process. The comprehensive investigation conducted by Gukendran et al. (2023) played a crucial role as a guiding reference. The extensive research conducted provided substantial evidence supporting the advantages of epoxy carbon fibre, therefore establishing it as the principal material for the present investigation.

Selection of Epoxy Carbon Woven (230 GPa)

Carbon fibres are renowned for their exceptional strength and stiffness characteristics, while epoxy resins serve the purpose of effectively bonding these fibres together. This bonding mechanism facilitates the transmission of stresses between the individual fibres, thus protecting them from any damage. The selection of epoxy carbon woven material was based on its fundamental qualities, particularly its outstanding modulus of elasticity, which measures 230 GPa. The blade's high rigidity guarantees its ability to withstand deformations in a range of operational situations. The utilisation of a woven structure, as opposed to unidirectional fibres, provides enhanced multidirectional strength, resulting in greater mechanical resilience against torsional and bending loads commonly seen in VAWT blade applications.

Criteria for the Initiation of Damage

The use of a stress-based damage start criterion was chosen due to the complexities involved with composite materials. The aforementioned criteria demonstrate a high degree of sensitivity towards the initiation of failure mechanisms, such as matrix cracking or fibre-matrix debonding. This characteristic renders it particularly pertinent in the context of epoxy carbon composites since these materials are prone to exhibiting such behaviours when subjected to complex loading conditions. (The detailed mechanical properties of Epoxy Carbon Woven (230 GPa) and damage criteria are presented in the Index section of this thesis.)

Layer Setup and Fibre Orientation

The configuration of the composite layer, specifically with regard to the orientation of fibres, was influenced by the research conducted by Boudounit, H., Tarfaoui, M., and Saifaoui, D. (2023). However, in the context of this thesis, it was considered necessary to minorly deviate from their method in order to overcome production restrictions and optimise resources. Instead of utilising the seven-ply structure, a more succinct five-ply configuration was implemented, with each individual ply measuring 0.2 mm in thickness with fibre orientation of -45, 0, 45, 0, -45. The aforementioned arrangement, although exhibiting variations in the number of plies and thicknesses, was designed to use the structural benefits revealed by Boudounit et al. (2023) while also ensuring feasibility in the manufacturing process. The decision to utilise lower thickness and a decreased number of plies was made with the explicit intention of simplifying the manufacturing process, hence enhancing the feasibility, cost-effectiveness, and scalability of VAWT blade production. The precise adjustment of the ply configuration exemplifies the essential equilibrium of empirical research, engineering feasibility, and production requirements.

Table 1 shows the entire layer setup including layer thickness and orientation angle of the material used for the blade in the Ansys Mechanical.

Table 1: Layer Orientations of Epoxy Carbon Woven (230 GPa)

Layer	Material	Thickness (mm)	Angle (°)
(+Z)			
5	Epoxy Carbon Woven (230 GPa) Wet	0.2	-45
4	Epoxy Carbon Woven (230 GPa) Wet	0.2	0
3	Epoxy Carbon Woven (230 GPa) Wet	0.2	45
2	Epoxy Carbon Woven (230 GPa) Wet	0.2	0
1	Epoxy Carbon Woven (230 GPa) Wet	0.2	-45
(-Z)			

Pre-Processing

Contact region and Coordination system

Ansys Mechanical includes several pre-processing steps before initiating the analysis of the inserted CAD model of the VAWT blades. Starting with the contact region, a bonded contact was made for the lap joints of the VAWT blades. It indicates that the lap joints exhibit a secure connection, characterised by the absence of slippage or any kind of relative movement between the jointed components.

Within the ANSYS software environment, the process of establishing this contact entails the careful selection of suitable surfaces for the contact pair. The 'Contact Shell Face' was chosen as the top of one of the adjacent components, while the 'Target Shell Face' was identified as the top of the other component. The utilisation of this configuration guarantees the precise assessment of stresses and deformations at the joint in the course of the study.

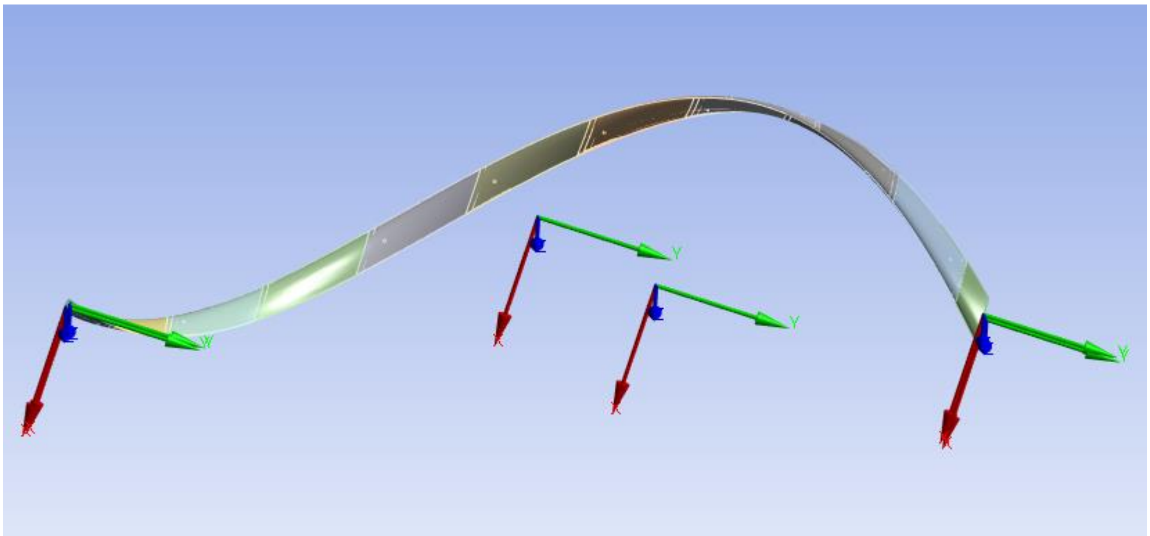

Figure 11: Various Coordination systems

The integration of diverse coordinate systems is crucial to simplify and optimise the implementation of loads and boundary conditions. Multiple coordinate systems have been created for the lap joint of the VAWT blade.

The primary coordinate system is a fundamental framework used to define and locate points in space. By default, the Global Coordinate System came into existence. All subsequent coordinate systems were established regarding this particular one. The Layer Orientation Coordinate System refers to a specific system used to define the orientation of layers in a given context. Situated at the centre of mass, this system was established to ensure the accurate orientation of the composite layers. This coordinate system's axes point in the same direction as the laminate's ply directions, making it easier to define material attributes and ply orientations. The development of distinct systems for individual load directions simplifies the process of applying load, hence eliminating the necessity for complex conversions or manipulations.

Figure 11 shows the implementation of these diverse coordinate systems which facilitated a structured methodology for establishing the model for analysis, thereby reducing the likelihood of mistakes and simplifying the succeeding stages of the process.

Meshing

The lap-joint analysis of the VAWT blades' meshing process was executed with extreme attention to detail to guarantee precise and dependable outcomes. A consistent meshing method was utilised over the whole blade geometry, with particular emphasis placed on the lap section. In this vital area, the mesh was further modified to improve the accuracy and reliability of the findings. To accomplish this objective, the Mapped Face Meshing method, a type of Sweep Meshing approach, was employed. This approach facilitates the management of element distribution, particularly in locations of significance, while maintaining the overall mesh quality in other areas.

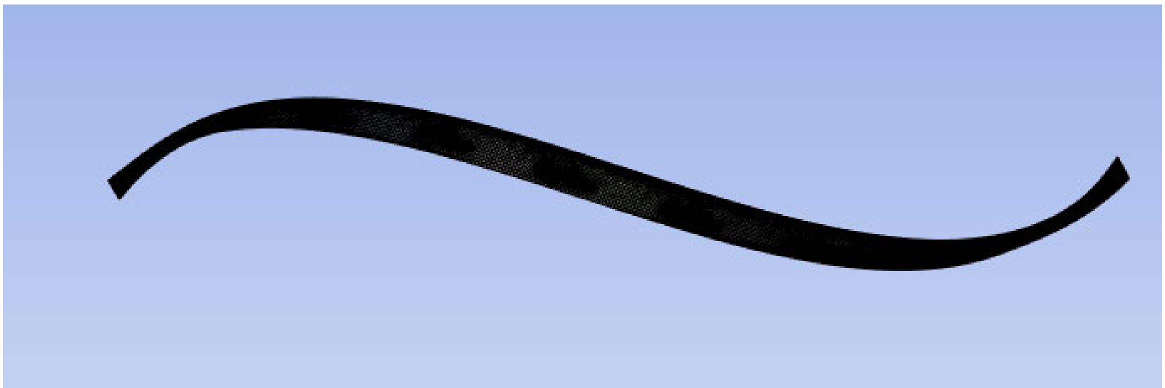

Figure 12: Refined Meshing of the Blade Assembly

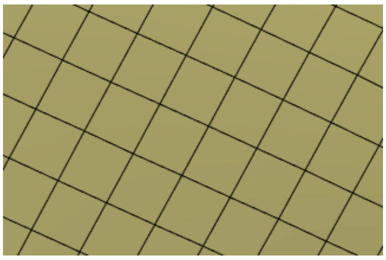

Figure 13: Enlarged View of the Mesh

In order to balance computational efficiency with the need for precise blade shape, a node merging technique was implemented. The aforementioned factor played a crucial role in reducing the overall quantity of elements and nodes, thereby enhancing the efficiency of the analysis process while maintaining the integrity of the outcomes. Figure 12 and Figure 13 show this refined mesh of the entire blade assembly which utilised an element size of 4.3124 mm, producing an overall count of 169,754 nodes and 172,065 elements. The implemented meshing approach not only guarantees the inclusion of all delicate elements of the blade's geometry in the finite element model but also assures a realistic representation of the actual physical behaviour of the lap joint of the VAWT blades under different load circumstances.

Loading Conditions

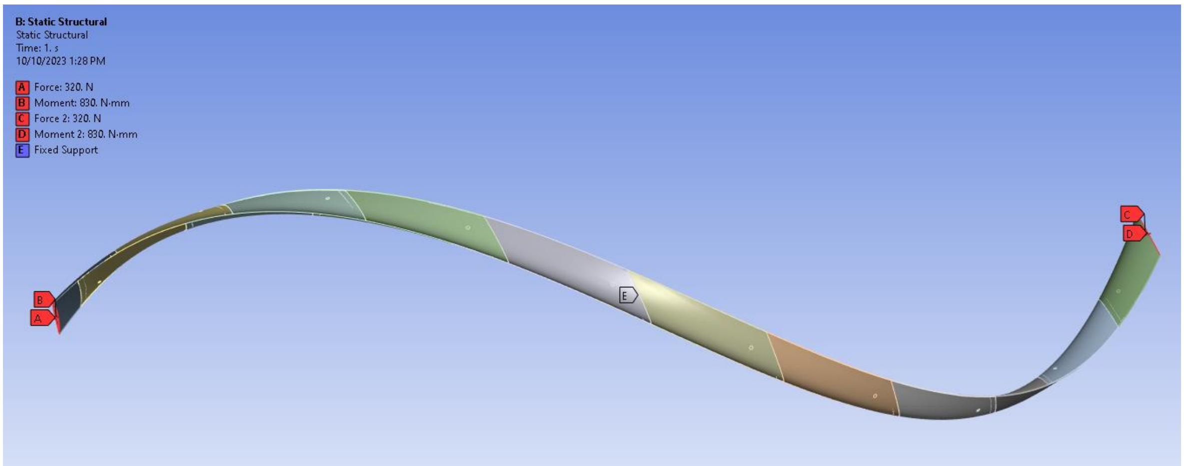

Figure 14:Applied loading conditions on the assembly

The accurate representation of real-world operational circumstances is crucial in this analysis of the lap joint of VAWT blades. This is vital to maintaining the precision of the finite element analysis. The trim portions of the first and final blades were subjected to two major loading situations, which are shown in Figure 14. Initially, a force of 320 N was exerted, which represents the inertia forces resulting from the blade's rotation. The centrifugal force resulting from the rotation of the blades exerts an outward radial force, which can have considerable effects on the structural integrity of the blade, particularly at the lap joint.

Table 2: Loading Conditions

Blade	Inertia Force	Bending Movement	Support
First trimmed Blade section	320 N	830 N.mm	-
Middle Blade Z-Section	-		Fixed Support
Last trimmed Blade section	320 N	830 N.mm	-

Furthermore, a bending moment of 830 N.mm. was applied in an edgewise downward direction, which is shown in Figure 14. The primary cause of the bending moment is attributed to aerodynamic forces, namely lift and drag, which exert their influence on the blade during its operational phase. The amplitude and direction of the forces exerted on the blade can be influenced by several factors, including the aerodynamic profile of the blade, its orientation, and the speed and direction of the incoming wind. In light of the blade's fundamental purpose of harnessing wind energy, it is essential to comprehend the impact of these aerodynamic forces to effectively optimise its design.

To simulate the boundary conditions, a fixed support was implemented on the z-section of the middle blade's face (Which is shown in detail in the appendices section of this thesis). The purpose of this constraint is to replicate the structural limitations experienced by the blades of a VAWT. By including these loading and boundary conditions shown in Table 2, it is ensured that the finite element analysis accurately represents the actual stresses and strains encountered by the VAWT blades, thereby enabling a more informed design optimisation process.

FEA Analysis

Engineers use FEA, a computational methodology, to predict and assess the mechanical response of materials and structures under various scenarios. In the context of static structural analysis, reviewing a VAWT blade lap joint involves the assessment of many significant factors and the study of failure criteria. The equations referred to by Ansys Mechanical in their programming are presented below for the specified parameters.

Equivalent Stress (von Mises Stress)

The von Mises stress is a measure of stress equivalence utilised to assess the initial stage of yielding in a material. If the maximum von Mises stress value remains below the yield strength of the material, it will not undergo yielding. The Von Mises stress can be determined by utilising either the stress components provided by the three-by-three stress tensor or by using the major stresses. Which is expressed by:

$$\sigma_{eq} = \sqrt{\frac{(\sigma_1-\sigma_2)^2+(\sigma_2-\sigma_3)^2+(\sigma_3-\sigma_1)^2}{2}} \quad \text{… (Eq 1)}$$

Where, $\sigma_1, \sigma_2, \sigma_3$ are principal stresses. (www.ansys.com, n.d.)

Equivalent Elastic Strain

There is an equivalent Von-Mises strain result in classical mechanics, just like there is an equivalent Von-Mises stress result. Additionally, Von Mises's stresses and outcomes are based on the same theories. However, ANSYS® Mechanical utilises an additional equation in their programming for solving Von-Mises strain findings for structural FEA simulations which can be represented as:

$$\varepsilon_{eq} = \frac{1}{1+v'}\sqrt{\frac{1}{2}[(\varepsilon_1 - \varepsilon_2)^2 + (\varepsilon_2 - \varepsilon_3)^2 + (\varepsilon_3 - \varepsilon_1)^2]} \quad \dots \text{(Eq 2)}$$

Where, $\varepsilon_1, \varepsilon_2, \varepsilon_3$ are principal strains and v' is Poisson's ratio. (Editor, 2021)

Maximum Shear Stress

The highest difference in orthogonal stresses within a material is measured as maximum shear stress. It stands for a significant variation in axial stresses in any orientation. Which can be expressed as:

$$\tau_{max} = \frac{\sigma_{max} - \sigma_{man}}{2} \quad \dots \text{(Eq 3)}$$

Where, σ_{max} *and* σ_{min} is maximum principal stress and minimum principal stress correspondingly. (Maximum Shear Stress: Theory & Formula Video, 2011)

Stress Intensity

The concept of intensity is commonly described as the highest magnitude of the discrepancy between the maximum and least primary stresses. In general, stress intensity is equivalent to double the value of the maximum shear stress. Which can be expressed as:

$$K = 2\tau_{max} \quad \dots \text{(Eq 4)}$$

Where, τ_{max} is Maximum Shear Stress (Editor, 2021).

Tai-Wu Failure Criterion

The maximum stress criteria that were employed earlier in this study are extended by the Tsai-Wu failure criterion, which gives a more comprehensive method that takes interaction effects into account. One notable attribute of this failure theory is its ability to differentiate between the tensile and compressive strengths, as demonstrated by Tsai-Wu. It is widely utilised in research due to its straightforward Ansys implementation.

The Tsai-Wu failure criterion can be mathematically expressed as a quadratic equation:

$$F_{11}\sigma_1^2 + F_{22}\sigma_2^2 + F_{66}\tau_{12}^2 + F_1\sigma_1 + F_2\sigma_2 + F_{12}\sigma_1\sigma_2 \leq 1 \quad \dots \text{(Eq 5)}$$

Where, $F_{11}, F_{22}, F_{66}, F_1, F_2, F_{12}$ are the strength tensors and σ_1, σ_2 & τ_{12} are the normal stresses.

According to Diniz et al.,(2019), The strength tensors can be calculated as follows:

$$F_{11} = \frac{1}{\sigma_1^T \sigma_1^C} \quad \dots \text{(Eq 6)}$$

$$F_{22} = \frac{1}{\sigma_2^T \sigma_2^C} \quad \dots \text{(Eq 7)}$$

$$F_1 = \frac{1}{\sigma_1^T} - \frac{1}{\sigma_1^C} \quad \dots \text{(Eq 8)}$$

$$F_2 = \frac{1}{\sigma_2^T} - \frac{1}{\sigma_2^C} \quad \dots \text{(Eq 9)}$$

$$F_{66} = \frac{1}{(\tau_{12}^F)^2} \quad \dots \text{(Eq 10)}$$

$$F_{12} \approx -\frac{1}{2}\sqrt{F_{11}F_{22}} \quad \dots \text{(Eq 11)}$$

Where T represents tensile factors and C represent compressive factors.

Using ANSYS Mechanical's Tsai-Wu failure criterion, a thorough failure analysis of both the original and optimised lap joint designs was performed. The Ansys Parametric Design Language (APDL), which enables a more thorough and customised analysis, was used to make this task simpler. (The coding scripts used for this method are included in the appendices.) This analytical method gave insights into the designs' structural integrity and potentially vulnerable locations, allowing for a comparison of the original and optimised versions.

RESULTS

FEA analysis was carried out on the various lap joint designs to select the best possible optimised design. For the simplicity of the thesis, only the initial and final selected design's FEA results are compared in this part of the thesis. This section analyses the variations between the original and the optimised designs of the lap-joint of the VAWT blades, focusing on five important variables derived from the Ansys static structural analysis:

- Equivalent stress (von Mises Stress)
- Equivalent Elastic strain
- Maximum shear stress
- Stress intensity
- Tsai-Wu failure

These five criteria were selected because, collectively, they offer a thorough insight into the structural behaviour and possible causes of failure of the VAWT blade lap joint. They guarantee that the joint will be robust and long-lasting under operational circumstances.

Equivalent Stress

Original Design

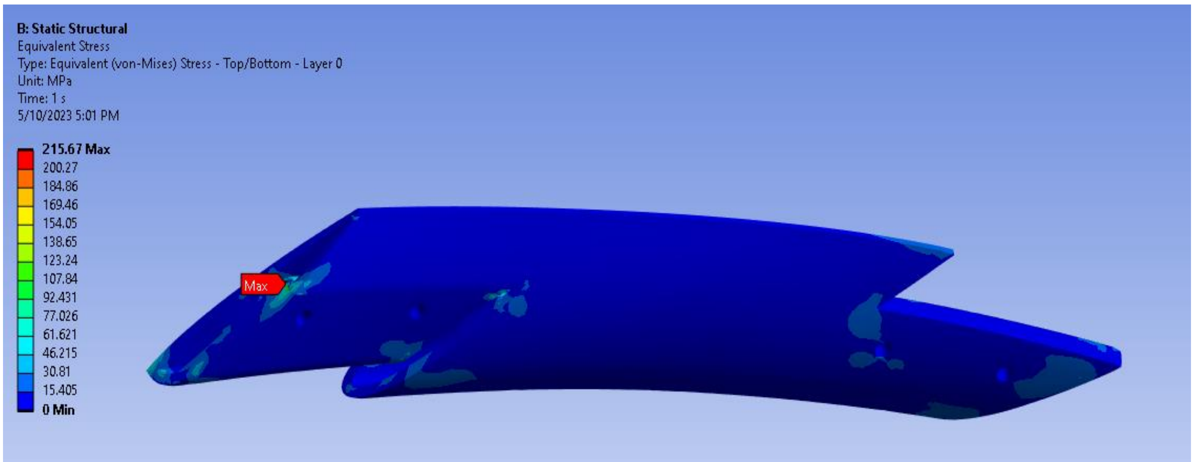

Figure 15: Equivalent Stress in Original Design

Optimised Design

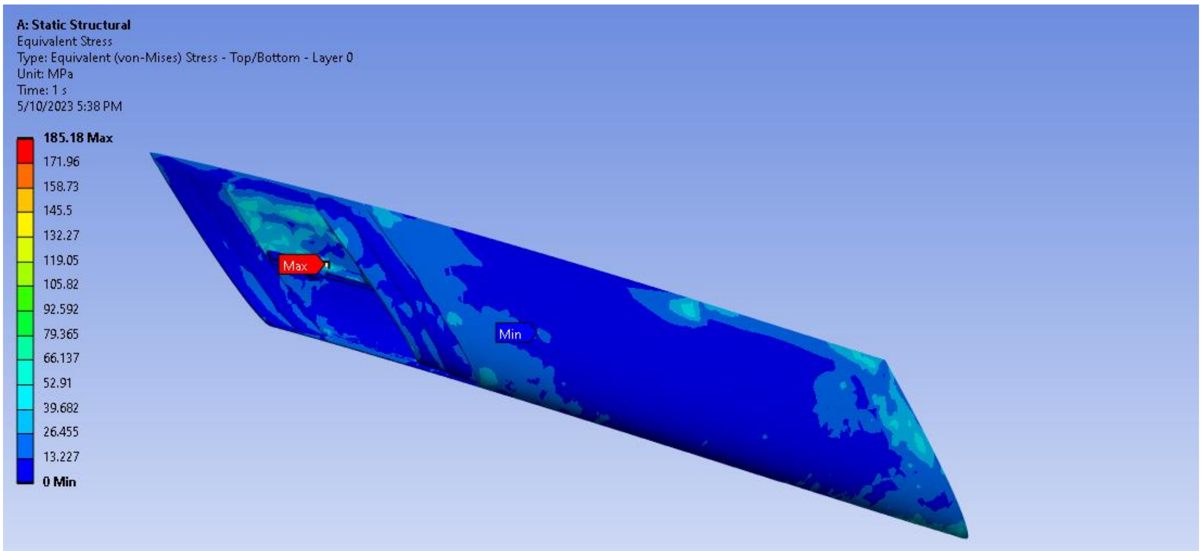

Figure 16: Equivalent Stress in Optimised Design

From Figure 15 and Figure 16, it can be seen that the blade's equivalent stress decreased from 215.67 MPa in the original design to 185.18 MPa in the optimised design, by around 14.1%. This suggests that the optimised design may more efficiently spread applied forces throughout its surface, leading to reduced stress concentrations.

Equivalent Elastic Strain

Original Design

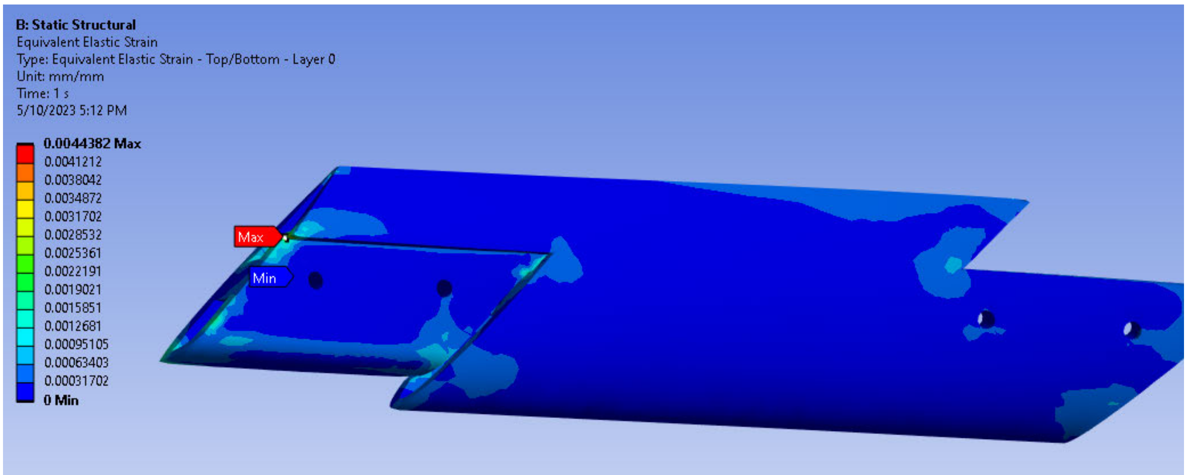

Figure 17: Equivalent Elastic Strain in Original Design

Optimised Design

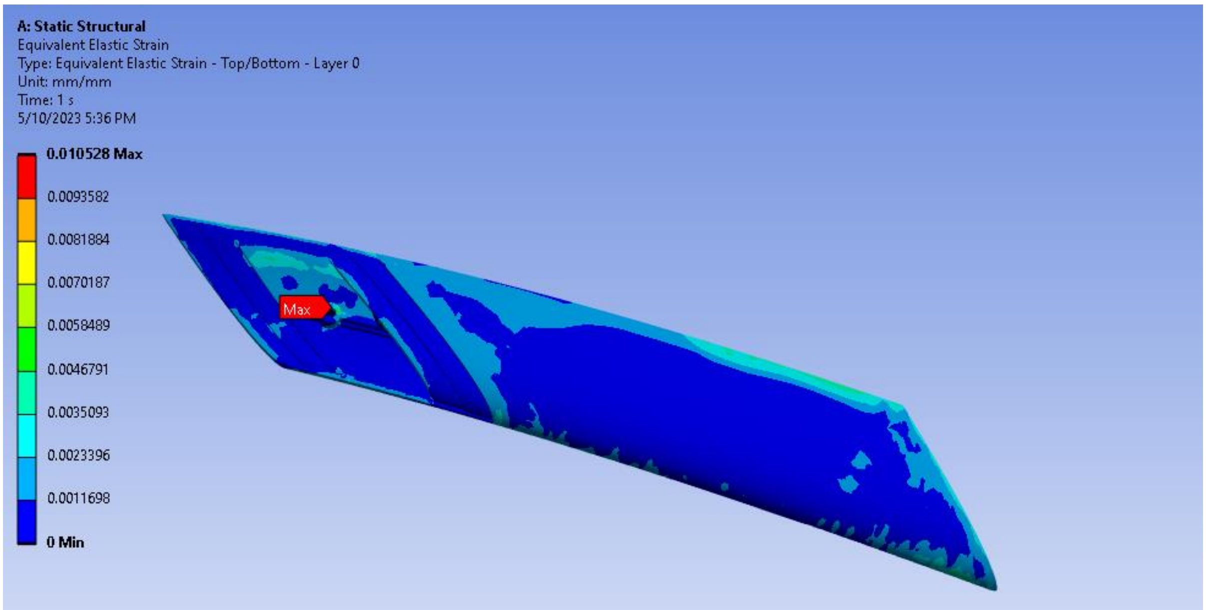

Figure 18: Equivalent Elastic Strain in Optimised Design

It's interesting to note that from Figure 17 and Figure 18, the equivalent strain in the optimised design went from 0.004438 mm/mm to 0.01052 mm/mm. This suggests that under comparable stress situations, the optimised design may experience larger deformations. However, if the material being used is ductile and can withstand stresses without affecting the integrity or performance of the blade, this increase in strain may be favourable.

Maximum Shear Stress

Original Design

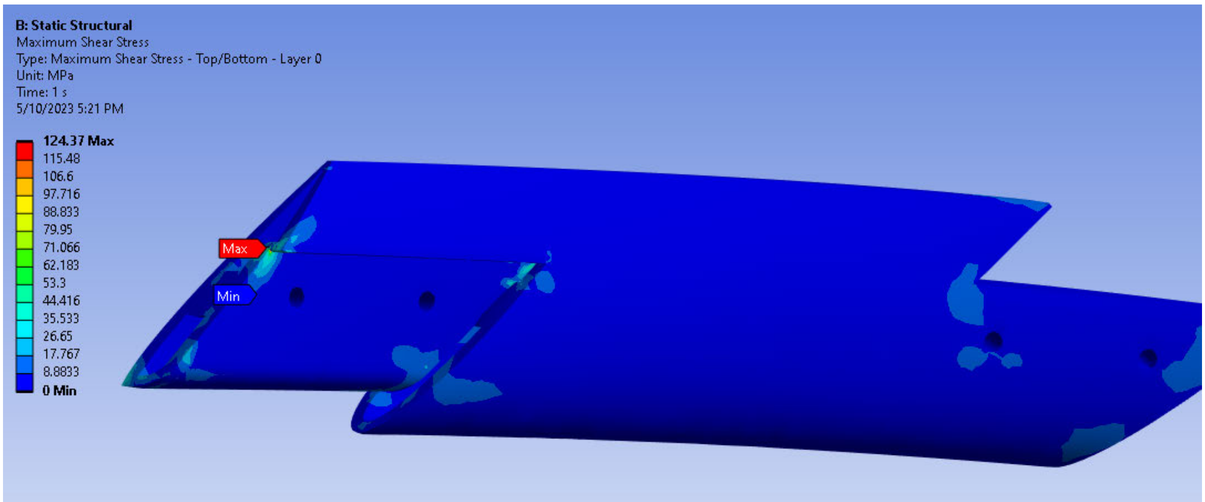

Figure 19: Maximum Shear Stress in Original Design

Optimised Design

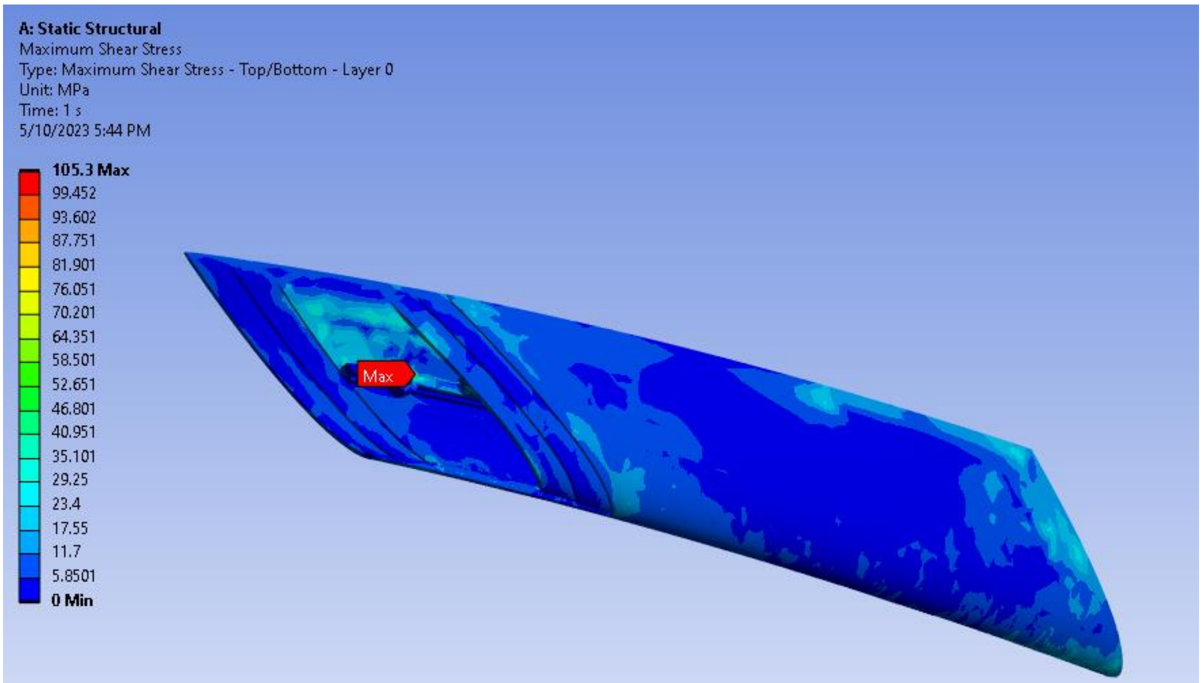

Figure 20: Maximum Shear Stress in Optimised Design

From Figure 19 and Figure 20, it can be seen that the maximum shear stress for the optimised design is decreased from 124.37 MPa to 105.3 MPa, a 15.3% reduction. A longer blade's lifespan and operating efficiency may be significantly increased by having reduced shear stress in the optimised design, indicating a higher capacity to withstand shearing forces.

Stress Intensity

Original Design

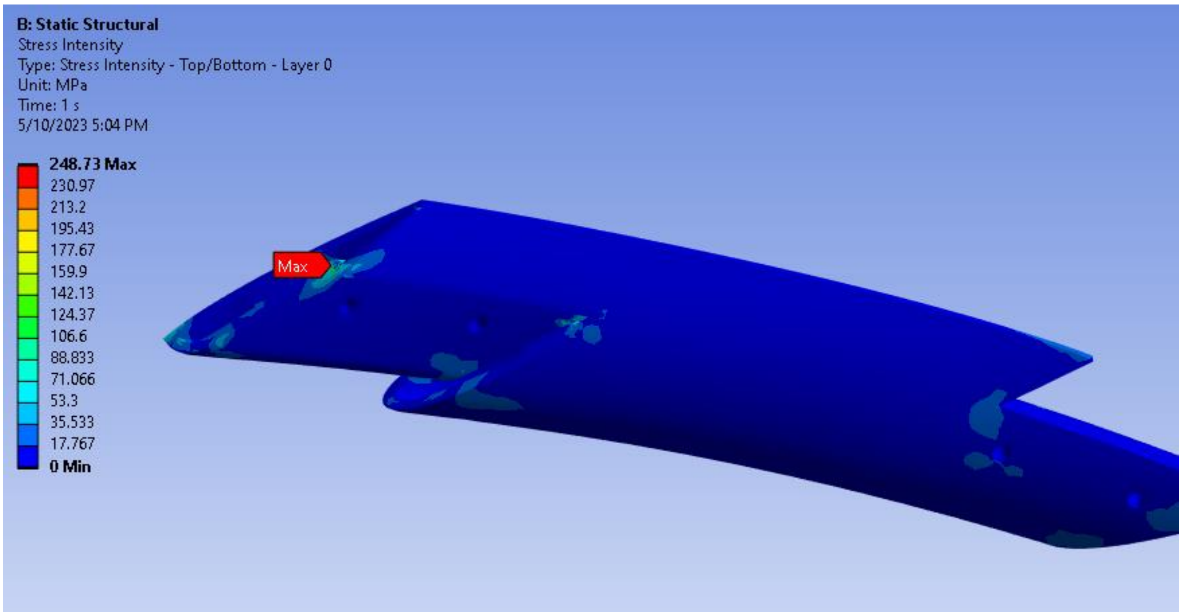

Figure 21: Stress Intensity in Original Design

Optimised Design

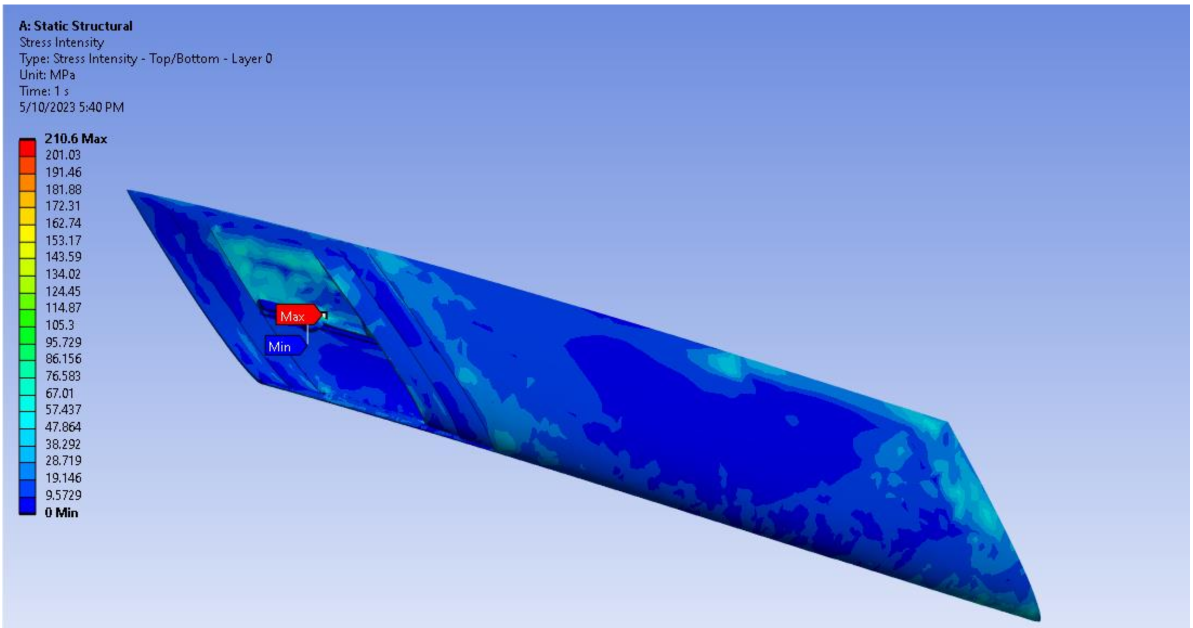

Figure 22: Stress Intensity in Optimised Design

Stress intensity is an indication of the possible propagation of fracture sites and severity. From Figure 21 and Figure 22, it can be seen that it has decreased from 248.73 MPa in the original design to 210.6 MPa in the optimised design. The optimised design may be less prone to fracture initiation and propagation as a result of this 15.3% decrease, increasing the blade's longevity and safety.

Tai-Wu Failure Criterion

Original Design

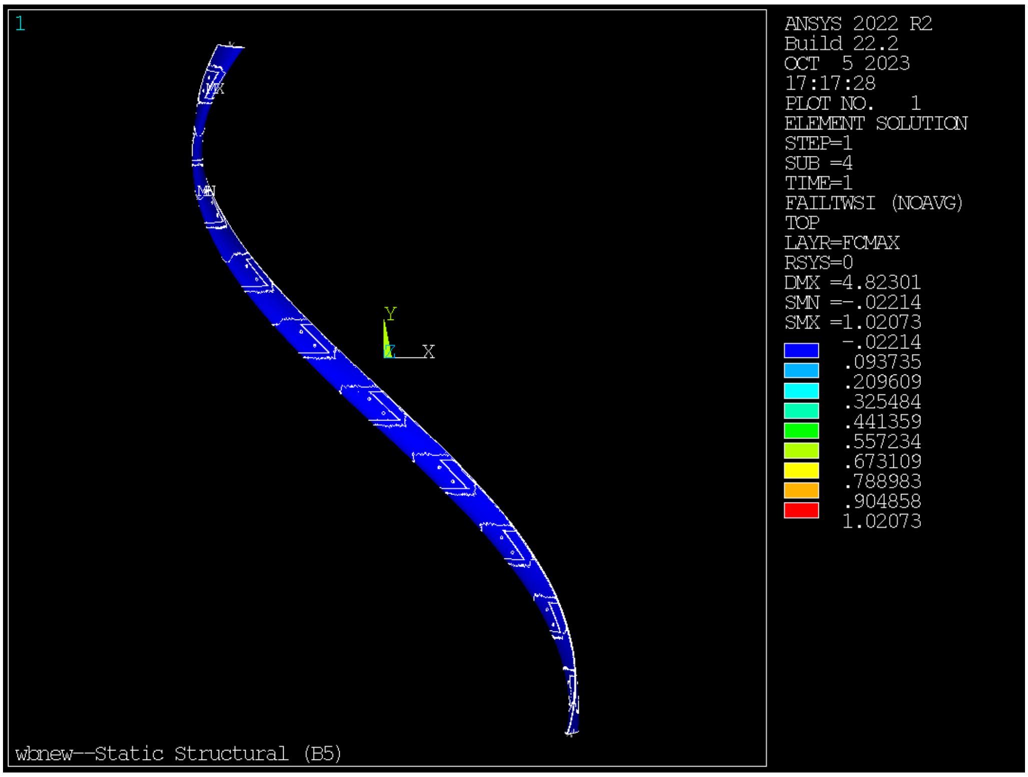

Figure 23: Tai-Wu Failure Criterion for Original Design

Optimised Design

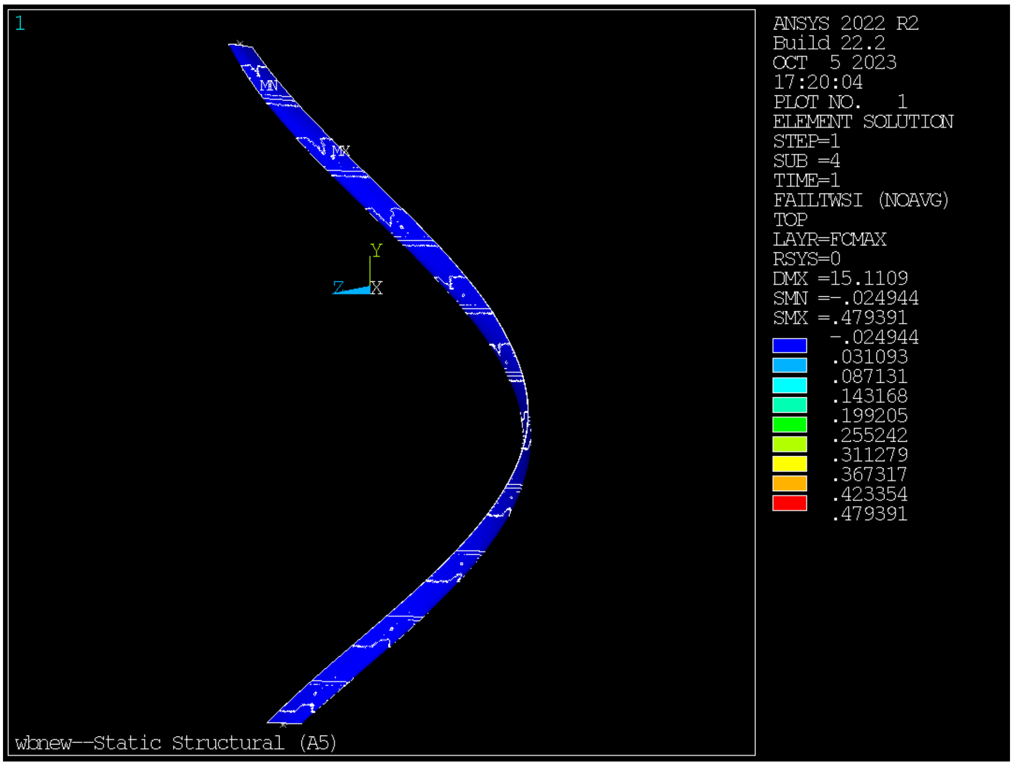

Figure 24: Tai-Wu Failure Criterion for Optimised Design

The Tsai-Wu failure criteria calculates the probability that a composite material will fail. The optimised design's value from Figure 24 is 0.479, which is significantly less than the original design's value of 1.020 from Figure 23. If the value is less than one, the design is safe since this criterion forecasts the margin of safety. The optimised design seems to have a much wider margin of safety against failure than the original due to the considerable decrease in the Tsai-Wu failure value.

Table 3: FEA Results

Mechanical Factors	**Original Design of Blade**	**Optimized Design of Blade**
Equivalent Stress	215.67 MPa	185.18 MPa
Maximum Shear Stress	124.37 MPa	105.3 MPa
Equivalent Strain	0.004438 mm/mm	0.01052 mm/mm
Stress Intensity	248.73 MPa	210.6 MPa
Tsai-Wu Failure	1.020	0.479

Table 3 shows that the optimised design of the VAWT blade's lap joint compares favourably in terms of stress distribution and resilience to failure modes. This demonstrates the efficiency of the design optimisation process and implies that the optimised design may provide superior performance, safety, and durability when compared to the original design.

DISCUSSION

Finite Element Analysis, which provides an in-depth understanding of the structural behaviours and responses of materials in various situations, is a crucial technique in design optimisation. With the use of FEA and the Epoxy Carbon Woven (230 GPa) material, this thesis produced an optimised design that shows substantial improvement over the original model.

Epoxy Carbon Woven's Material Behaviour

Epoxy Carbon Woven has exceptional stiffness and durability against deformation due to its high 230 GPa modulus of elasticity. Due to these properties, the material is a great choice for applications like wind turbine blades, where preserving structural integrity while guaranteeing a high strength-to-weight ratio is crucial. However, the configuration of the material is equally as important to its performance as its intrinsic qualities. The orientation of fibre angles of -45, 0, 45, 0, -45 degrees has provided a balanced resistance to torsion and bending forces. The design successfully utilises the anisotropic features of the composite material by aligning the fibres in this order. Along the main axis of the blade, this orientation provides advantages such as a reduced maximum shear stress of 105.3 MPa from 124.37 MPa, improving structural integrity and endurance.

Stress Distribution

The major benefit of the optimised design is the improved stress distribution. The optimised blade demonstrates its enhanced capacity to support and distribute loads with stress intensity lowered to 210.6 MPa from 248.73 MPa. Moreover, the optimisation process highlighted the shifting of wuulant stress. The equivalent stress in the original model, recorded at 215.67 MPa, was mostly along the lap edges, a major design weakness. The optimised design has successfully diverted these intensities to the z-section, encouraging a more even and secure stress distribution with an equivalent stress of 185.18 MPa, which can be seen in Figure 25.

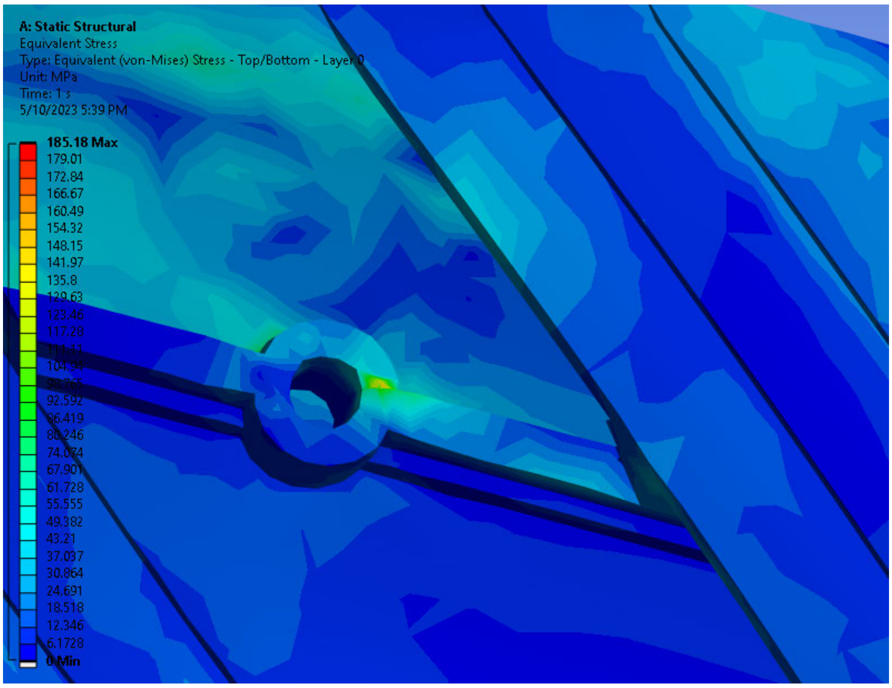

Figure 25: Enlarged View of Equivalent Stress at the Z-section of the lap

Enhanced Safety with Tsai-Wu Failure Criteria

A crucial tool for evaluating anisotropic materials like composites, the Tsai-Wu failure criteria provide a thorough prediction of probable material failure under multi-axial loading. The optimised design's significantly lower Tsai-Wu value (0.479 as opposed to the original's 1.020) indicates a substantially higher safety margin. This safety margin results in a more durable blade, lowering the possibility of unanticipated catastrophic failures.

Longer Blade Life

Reduced stress concentrations and improved stress distribution directly lead to the blade's increased lifetime. The blade requires fewer maintenance interventions since stress is reduced across many operating cycles, resulting in a longer operational life for the VAWT blades.

FEA Analysis and Relevance

This research provides a full understanding of structural behaviours through the lens of FEA. In the case of the VAWT blade, FEA highlighted the original design's weak points and potential improvement areas. The optimised design's stress intensity transition from the lap edges to the z-section beam is evidence of the valuable insights provided by FEA. FEA guarantees that design optimisation is grounded in empirically supported data by modelling real-world situations, bringing designs closer to real-world perfection.

VALIDATION AND VERIFICATION

The result of the FEA analysis was validated through experiential testing of the blades' optimised design assembly. Due to limited resources, the experimental testing was done on a three-blade assembly rather than an eleven-blade assembly. However, the entire methodological process of the FEA analysis was kept the same as the eleven-blade assembly to get as accurate validation as possible. (This experimental testing was done by a fellow student who is working under a similar VAWT-X project named "Design, Development, and Strain Measurement System for VAWT.")

Experimental Methodology

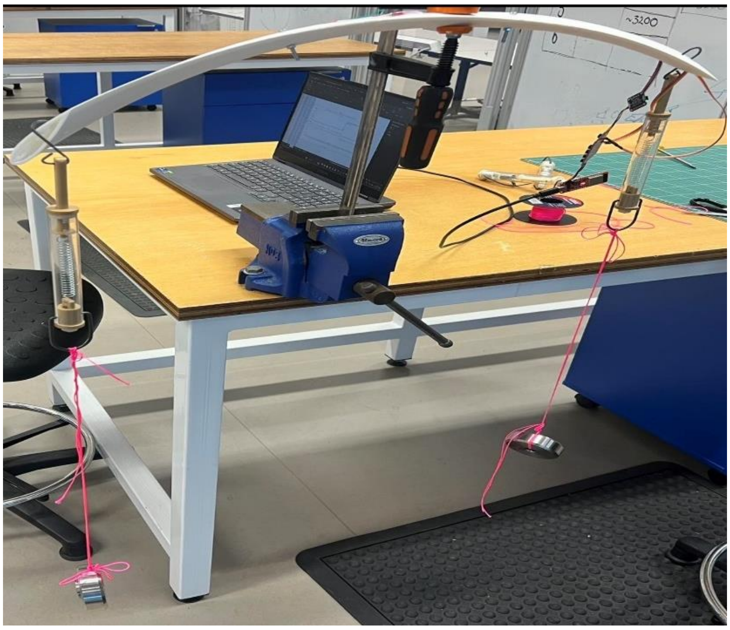

Figure 26: Experimental Set-Up of 3 Blades Assembly

(Source: Design, Development and Strain Measurement System for VAWT blades by Deepak Sapkota)

Three hollow blades that have been glued together served as the test model for the experimental static analysis, which can be seen in Figure 26. On the surface of the blade, rectangular strain gauges were carefully attached to form quarter bridge circuits. These bridge systems were linked via the analogue-to-digital converters (ADCs) placed inside the hollow cavity, which were then connected to a multiplexer and transmitted information to a microcontroller. The digital strain signals were captured using the Arduino platform. For testing in experiments:

- The model's sideways hole was subjected to 3.5 N, 8.5 N, 10.5 N, 12 N and 17 N loads on both ends for creating five different scenarios, keeping fixed support on the right side of the strain gauge, especially at the lap joint area.
- The experimental results for each different load are mentioned in Table 4.

Table 4: Experimental Results for Various Loads

(Source: Design, Development and Strain Measurement System for VAWT blades by Deepak Sapkota)

Loads	Maximum Shearing Stress (MPa)	Stress Intensity(MPa)
3.5N	0.424	0.848
8.5N	0.914	1.828
10.5N	1.3	2.6
12N	1.431	2.862
17N	1.731	3.462

FEA Analysis Using ANSYS

A 3D CAD model that replicates the actual geometry of the three-blade assembly was created. Polylactic acid (PLA) material was inserted in the Ansys workbench which was the exact material from which the optimized blade was 3D printed. Sweep meshing and the mapped face meshing technique were both used to mesh this model. Given the importance of accurately representing stress, mesh refinement specifically targeted high-stress concentration regions like holes. The centre blade lap section was provided with fixed support, indicating a limitation in its degrees of freedom and forbidding any movement. The remaining blades were free to move but had loading conditions applied to their holes. Five different scenarios were taken into account for loading Conditions as per the experimental method:

- On the first and last blade holes, 3.5 N, 8.5 N, 10.5 N, 12 N and 17 N loads were applied keeping similar to the experimental method. The loading condition for 17 N can be seen in Figure 27. (The rest of the loading conditions are presented in the appendices section of this thesis.)

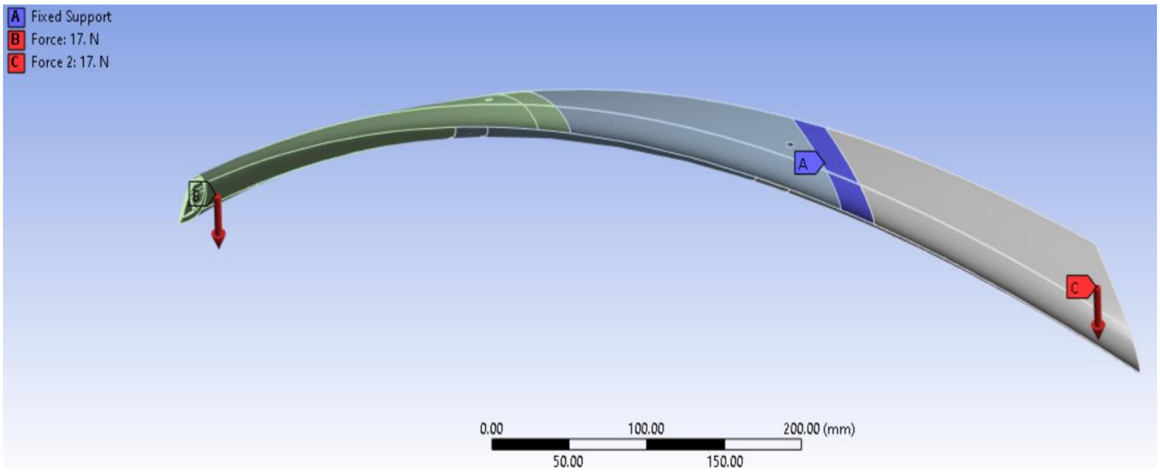

Figure 27:Loading Conditions (17 N)

Results

To validate the FEA results, Maximum Shear Stress and Stress Intensity were chosen because validating the accuracy and reliability of these two parameters can establish a solid basis for future FEA investigations. Once the FEA model has proven its capability to reliably anticipate Maximum Shear Stress and Stress Intensity, it may be utilised or modified for further studies, even in the absence of immediate experimental data for those parameters.

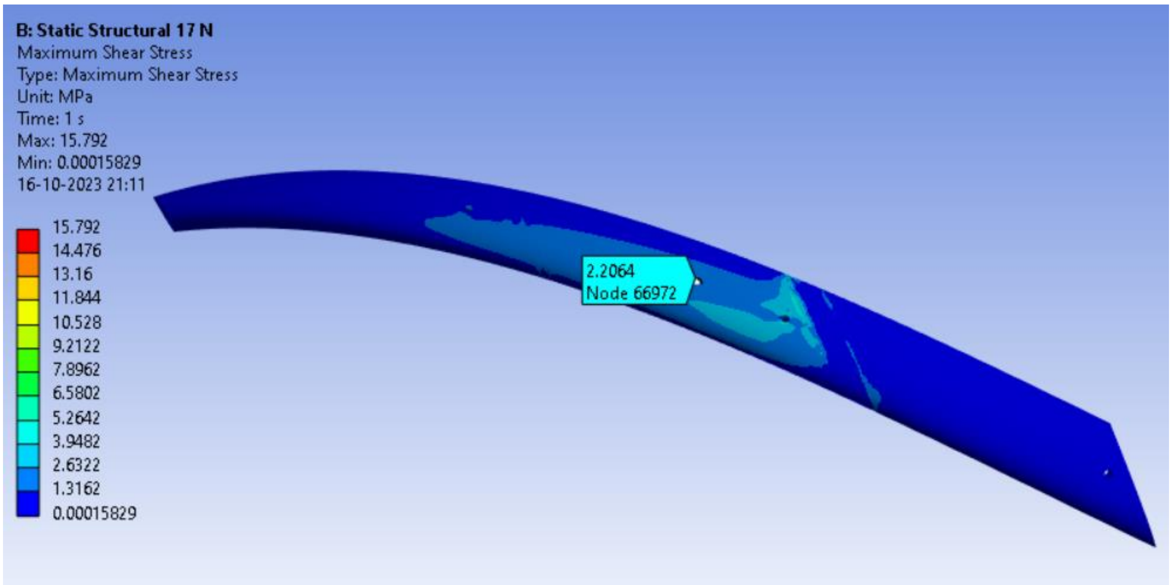

Figure 28: Maximum Shear Stress at a particular location

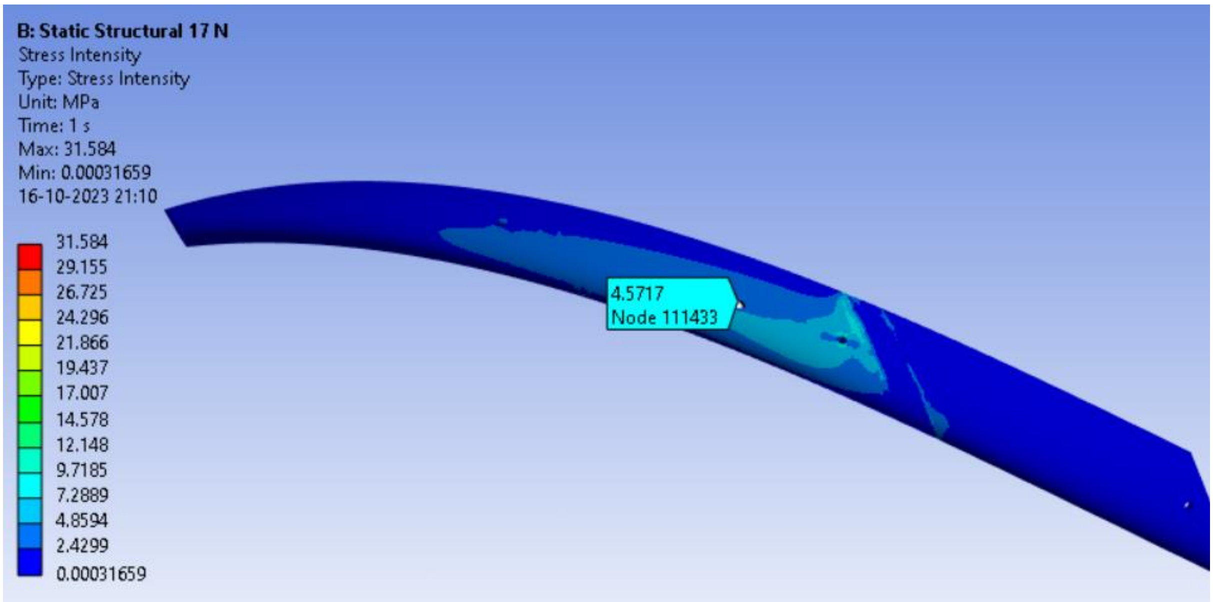

Figure 29: Stress Intensity at a particular location

For a 17 N load, the applied force and the restrictions on the central blade resulted in a computed maximum shear stress and stress Intensity at the exact location as the experimental one was measured: 2.2064 MPa and 4.5717 MPa which can be seen in Figures 28 and 29 respectively. (The rest of the results for different loads are presented in the appendices section of this thesis.)

Results Validation

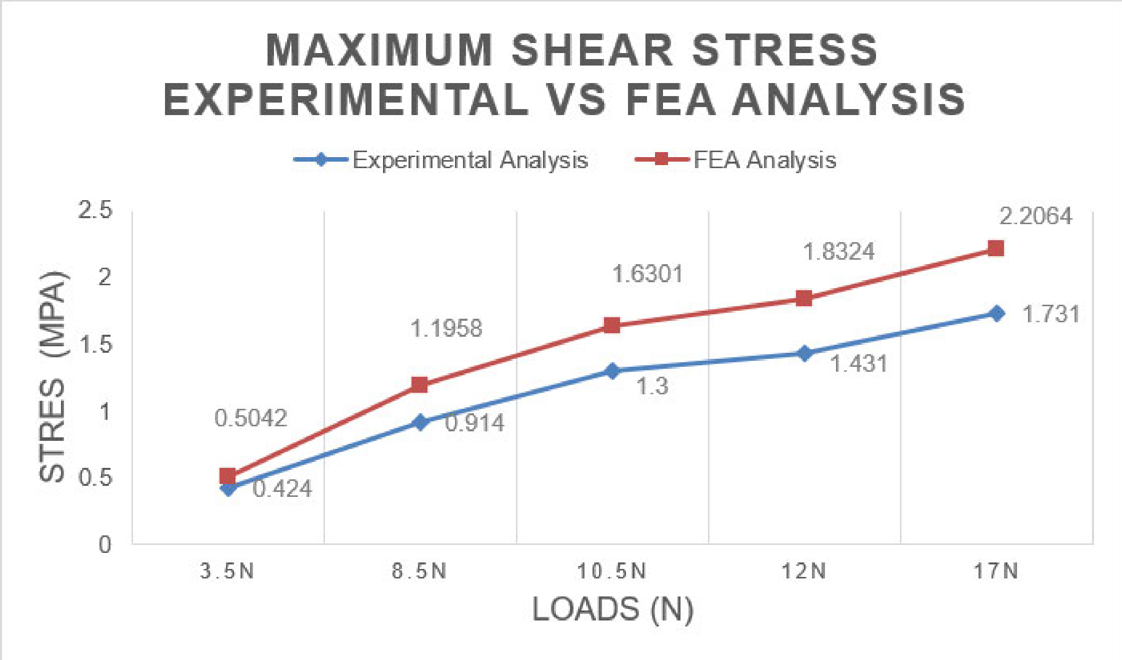

Figure 30: Results comparison for Maximum Shear Stress

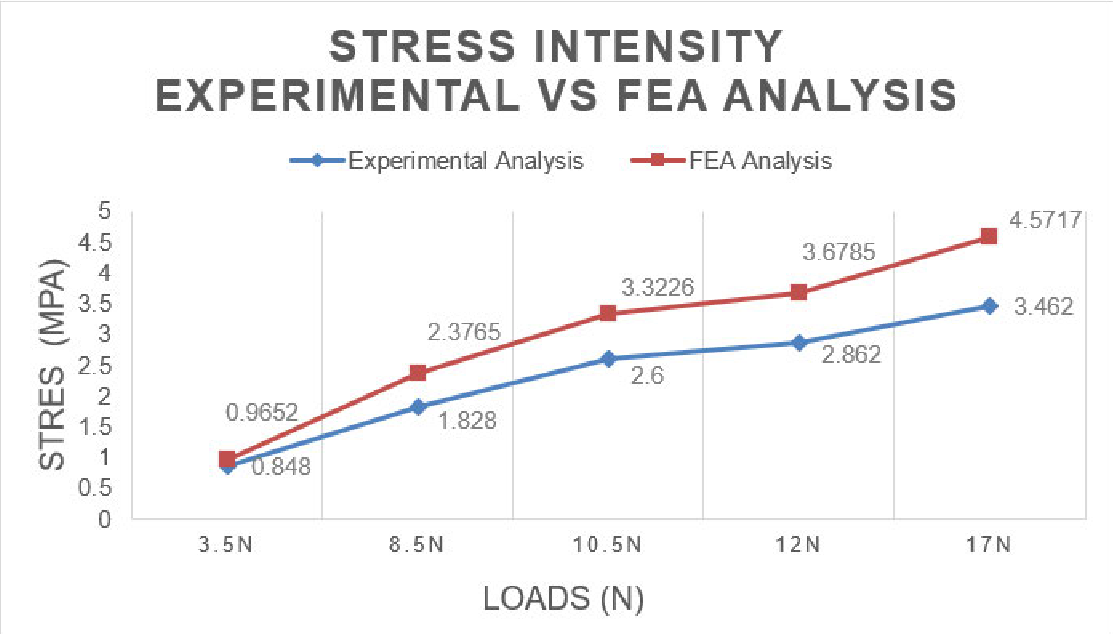

Figure 31: Results comparison for Stress Intensity

From Figures 32 and 33, A clear linear pattern of progression is seen with the increase in load when closely examining the graphs comparing experimental and FEA results for maximum shear stress and stress intensity. This linear trend in the experimental and FEA data points to a proportional link between the applied load and the measured stress levels. According to the linear progression, the material behaviour, as represented by both the experimental technique and the FEA model, is constant under different loads. It supports the idea that the FEA model accurately depicts the material's basic mechanical behaviour and its reaction to the applied loads. Table 5 of percentage discrepancies between the experimental and FEA findings provide more insight.

Table 5: Average Difference Experimental & FEA Results

Mechanical Factors	**3.5N**	**8.5N**	**10.5N**	**12N**	**17N**	**Average% Difference**
Maximum Shear Stress	18.9%	30.8%	25.4%	28.1%	27.4%	**26.1%**
Stress Intensity	13.8%	30.0%	27.8%	28.6%	32.0%	**26.4%**

The percentage differences for each unique load value exhibit a consistent trend, as seen in the table. Although there are differences between the experimental and FEA results, these differences are largely constant for various loads. The average percentage differences—which are 26.1% for maximum shear stress and 26.4% for stress intensity—further demonstrate this homogeneity.

In conclusion, both experimental and FEA findings exhibit a similar linear trend in response to increasing loads on the graphical representation. The constant percentage deviations and uniform trends shown across various load values further demonstrate the accuracy of the FEA model in modelling the mechanical behaviour of the material. The average percentage difference is constant; however, the value difference might be due to the misalignment or miscalibration of the ADCs and associated equipment, which can cause systematic errors. The Arduino's sampling rate constraints may result in the omission of quick changes in strain signals, which might cause inconsistencies in the experimental setup. Also, the assumptions made in the FEA model regarding material qualities and boundary conditions may have affected the final results.

Such validation provides insight into the assembly's durability and robustness under such loadings, particularly when compared to the material's tolerance limits. This comparison analysis highlights how reliable the FEA approach is in this thesis. The primary 11-blade assembly FEA analysis, which is the thesis' main focus, is strengthened by these insights into the behaviour of the 3-blade assembly.

FUTURE WORK

Future research might explore a number of directions to improve and further enhance the design and functionality of VAWT blades, including:

- **Fatigue Analysis:** Given the fact that wind turbines experience several cyclic loads over their operational lifespan, conducting a comprehensive fatigue analysis can prove advantageous. This analysis could provide valuable insights regarding the long-term performance of the blade and any deterioration that may occur over the course of its lifespan.
- **Thermal analysis:** It plays a crucial role in understanding the behaviour of VAWT blades under varying climatic circumstances. By investigating the thermal loads and performance of the lap-joint design at different temperature levels, useful insights can be gained.
- **Scale-up Analysis:** The next logical progression in this analysis would include scaling up the optimised design to accommodate the Darrieus VAWT from VAWT-X Energy. The examination of feasibility, performance, and structural behaviours on a larger scale can offer valuable insights into their practical applications in real-world scenarios.

By incorporating these aspects into future research, the improvement of VAWT blade designs can be advanced to new heights, thereby offering more effective, environmentally friendly, and dependable alternatives for renewable energy generation.

CONCLUSION

This study has effectively shown the significant influence of design optimisation on the durability VAWT blade's lap joint. By utilising a reliable FEA in ANSYS, the study successfully identified the flaws in the original design and provided insights into the direction for developing an enhanced and optimised version. The optimised VAWT blade lap-joint design shows noticeable superiority over its original counterpart by combining the complex insights of FEA with the distinctive characteristics and orientations of the Epoxy Carbon Woven material. The thesis's key discovery points to a notable improvement in the optimised design's stress distribution over the original model. In the original design, a major design weakness was identified by a high-stress intensity of 248.73 MPa that was mostly seen around the lap edges, which can be the initial failure point. However, with the introduction of the optimized design, the stress intensities were effectively redirected to the z-section beam. With a lower stress intensity at 210.6 MPa, this redirection achieved a more even and stable stress distribution. Overall, the optimised blades' lap joint design provides better stress distribution, lower stress intensities, improved safety margins according to the Tsai-Wu failure criteria, and the possibility of a longer operating lifespan. Such proficient optimisations will be essential to ensuring the effectiveness and durability of systems like VAWTs as the field of renewable energy develops.

BIBLIOGRAPHY

ARCADIA (2017). *Vertical Axis Wind Turbines Advantages & Disadvantages*. [online] blog.arcadia.com. Available at: https://blog.arcadia.com/vertical-axis-wind-turbines-advantages-disadvantages/.

Vawt-X Energy. (n.d.). *Features*. [online] Available at: https://vawt-x.com.au/features/ [Accessed 11 Oct. 2023].

Kupski, J. and De Freitas, S.T., 2021. Design of adhesively bonded lap joints with laminated CFRP adherends: Review, challenges and new opportunities for aerospace structures. *Composite Structures*, *268*, p.113923.

Chen, P.I., Wang, K.Y. and Huang, H.H., 2019. Strength and failure modes of adhesively bonded composite joints with easily fabricated nonflat interfaces. *Composite Structures*, *225*, p.111162.

Lindkvist, O. and Nicolausson, V., 2019. Design of wind turbine blades with respect to stability. *TVSM-5000*.

Gukendran, R., Sambathkumar, M., Sabari, C., Raj, C.R. and Kumar, V.R., 2022. Structural analysis of composite wind turbine blade using ANSYS. *Materials Today: Proceedings*, *50*, pp.1011-1016.

Yeh, M.K. and Wang, C.H., 2017, October. Stress analysis of composite wind turbine blade by finite element method. In *IOP Conference Series: Materials Science and Engineering* (Vol. 241, No. 1, p. 012015). IOP Publishing.

Boudounit, H., Tarfaoui, M. and Saifaoui, D., 2023. Fatigue analysis of wind turbine composite blade using finite element method. Wind Engineering, 47(3), pp.706-721.

Salimi-Majd, D., Azimzadeh, V. and Mohammadi, B., 2015. Loading analysis of composite wind turbine blade for fatigue life prediction of adhesively bonded root joint. *Applied Composite Materials*, *22*, pp.269-287.

Diniz, C.A., Cunha, S.S., Gomes, G.F. and Ancelotti, A.C., 2019. Optimization of the layers of composite materials from neural networks with Tsai–Wu failure criterion. *Journal of Failure Analysis and Prevention*, *19*, pp.709-715.

www.ansys.com. (n.d.). *What is Equivalent Stress?* [online] Available at: https://www.ansys.com/blog/what-is-equivalent-stress.

Editor, M.E.C. (2021). *Equivalent Strain Solution In ANSYS® Structural Analyses*. [online] ML - Best Engineering Blog. Available at: https://mechanicalland.com/equivalent-strain-solution-in-ansys-structural-analyses/ [Accessed 12 Oct. 2023].

Editor, M.E.C. (2021). *Stress And Strain Intensity Results In ANSYS® Structural Analyses*. [online] ML - Best Engineering Blog. Available at: https://mechanicalland.com/stress-and-strain-intensity-results-in-ansys-structural-analyses/ [Accessed 12 Oct. 2023].

Maximum Shear Stress: Theory & Formula Video (2011). *Maximum Shear Stress: Theory & Formula - Video & Lesson Transcript* | *Study.com*. [online] Study.com. Available at: https://study.com/academy/lesson/maximum-shear-stress-theory-formula.html.

APPENDICES

1. **Optimised Design Engineering Drawing (Source: Design Automation of Manufacturing process for VAWT Blade & its Mould by Parametrization by Nitesh Poudel)**

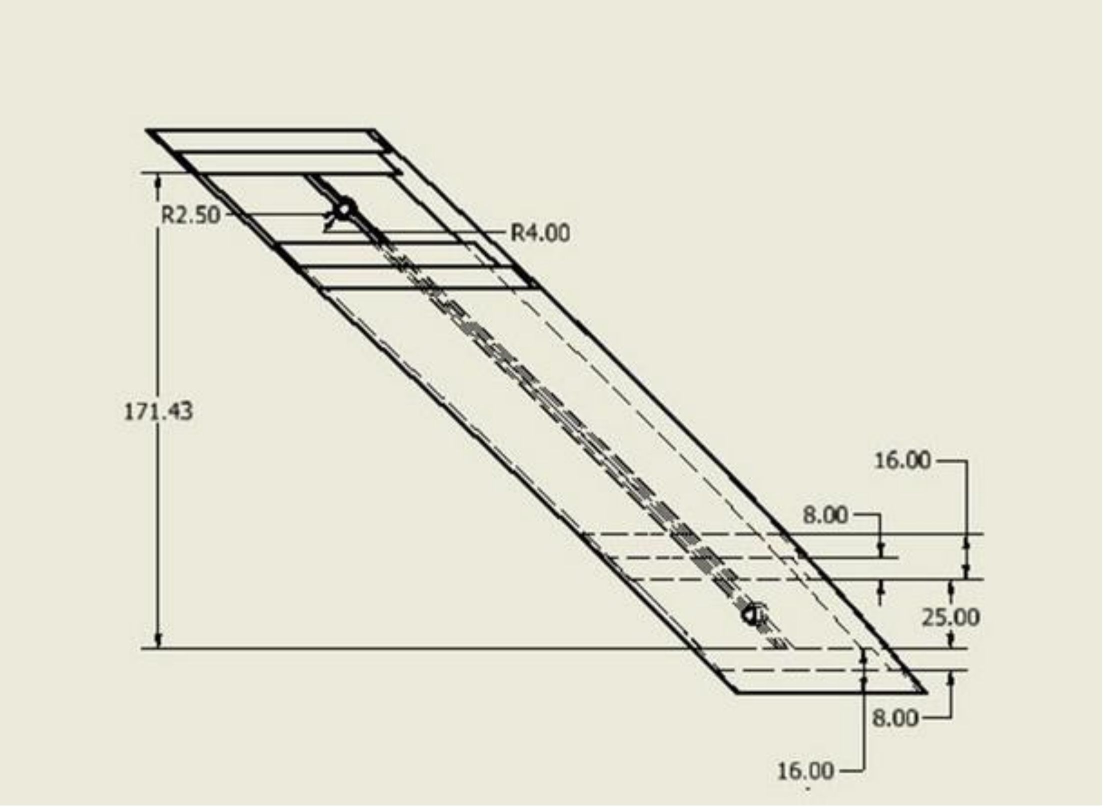

2. **Various Lap joint designs go through FEA before coming to the final optimised Design (Source: Design Automation of Manufacturing process for VAWT Blade & its Mould by Parametrization by Nitesh Poudel)**

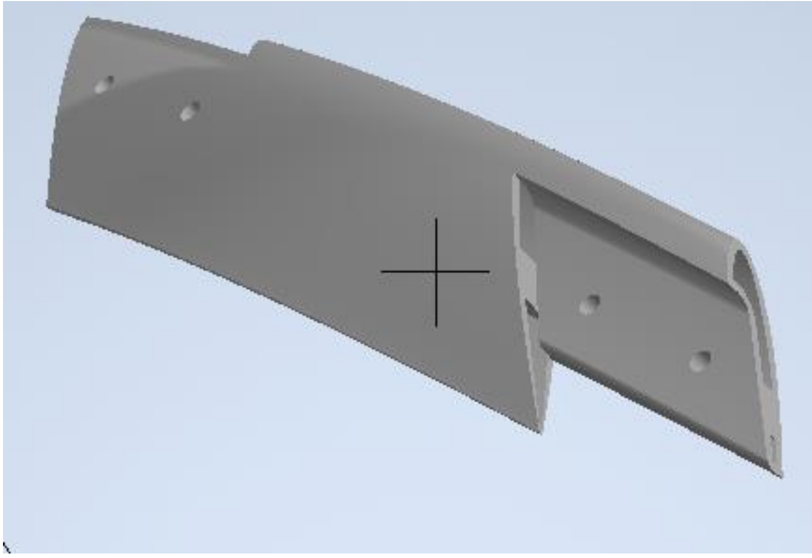

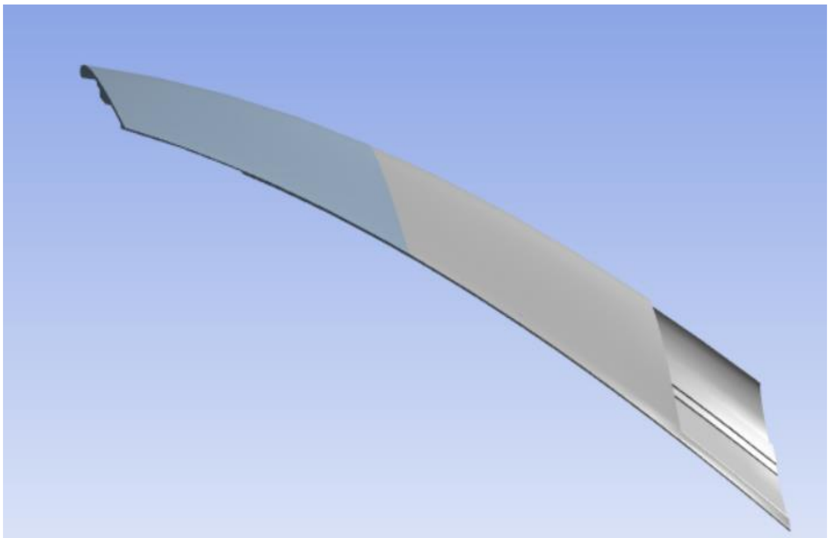

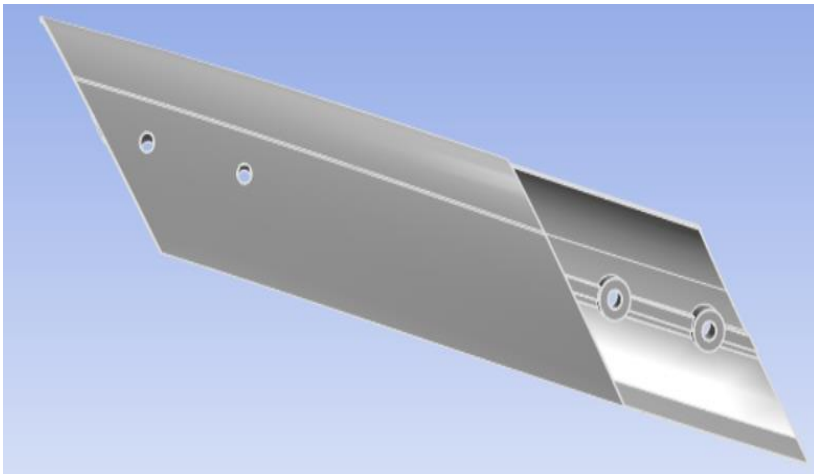

3. Ansys ADPL command programming of Tsai-Wu Failure Criterion

Commands

```
! Commands inserted into this file will be executed immediately after the ANSYS /POST1 command.

! Active UNIT system in Workbench when this object was created:  Metric (mm, kg, N, s, mV, mA)
! NOTE:  Any data that requires units (such as mass) is assumed to be in the consistent solver unit system.
!               See Solving Units in the help system for more information.


set,last
layer,fcmax
/show,png
/view,0,0,1
plesol,fail,twsi
```

4. Epoxy Carbon Woven (230 GPa)

Properties of Outline Row 3: Epoxy Carbon Woven (230 GPa) Wet

	A	B	C
1	Property	Value	Unit
2	Density	1451	kg m^-3
3	Orthotropic Secant Coefficient of Thermal Expansion		
8	Orthotropic Elasticity		
9	Young's Modulus X direction	5.916E+10	Pa
10	Young's Modulus Y direction	5.916E+10	Pa
11	Young's Modulus Z direction	7.5E+09	Pa
12	Poisson's Ratio XY	0.04	
13	Poisson's Ratio YZ	0.3	
14	Poisson's Ratio XZ	0.3	
15	Shear Modulus XY	3.3E+09	Pa
16	Shear Modulus YZ	2.7E+09	Pa
17	Shear Modulus XZ	2.7E+09	Pa
18	Orthotropic Stress Limits		
28	Orthotropic Strain Limits		
38	Tsai-Wu Constants		
39	Coupling Coefficient XY	-1	
40	Coupling Coefficient YZ	-1	
41	Coupling Coefficient XZ	-1	
42	Damage Initiation Criteria		
43	Tensile Fiber Failure Mode	Maximum Stress	
44	Compressive Fiber Failure Mode	Maximum Stress	
45	Tensile Matrix Failure Mode	Maximum Stress	
46	Compressive Matrix Failure Mode	Maximum Stress	
47	Damage Evolution Law		

5. Trimmed section of the optimised blade

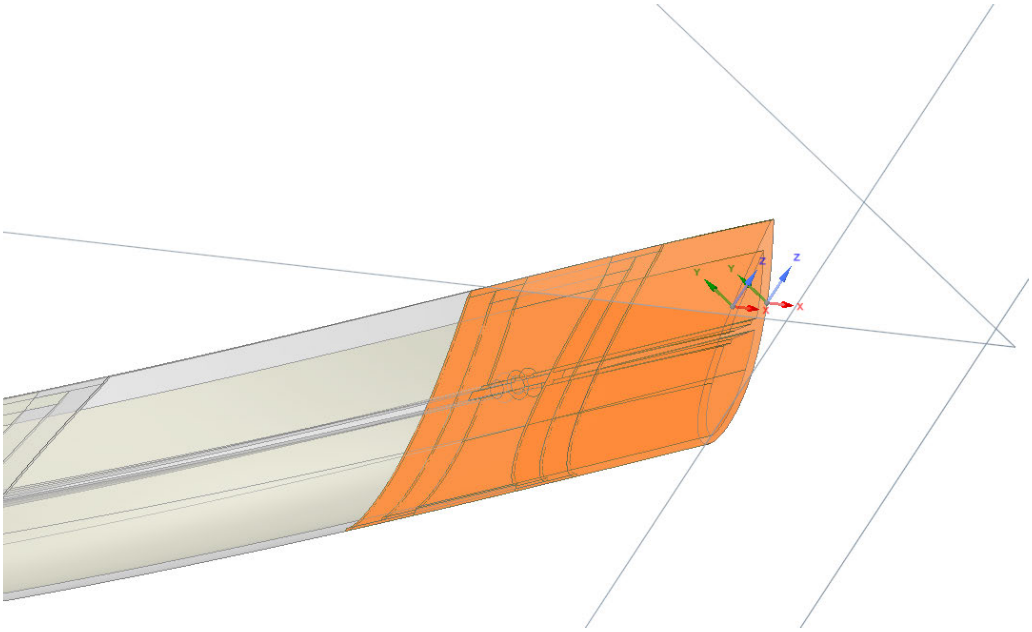

6. Loading Condition direction

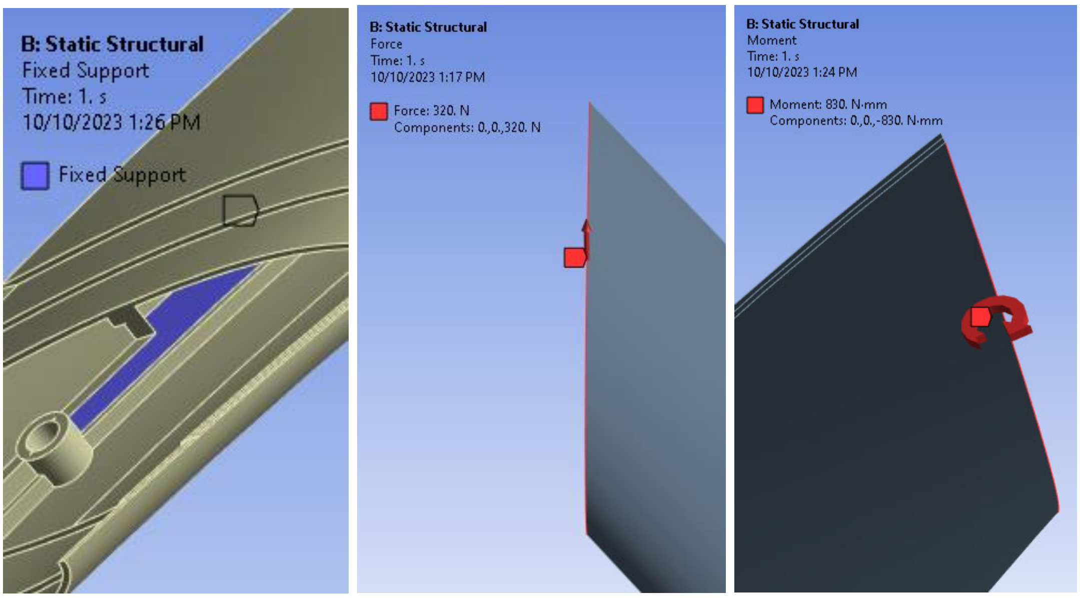

7. Enlarge View of Optimised Blade’s Lap Joint Showcasing Stress Intensity

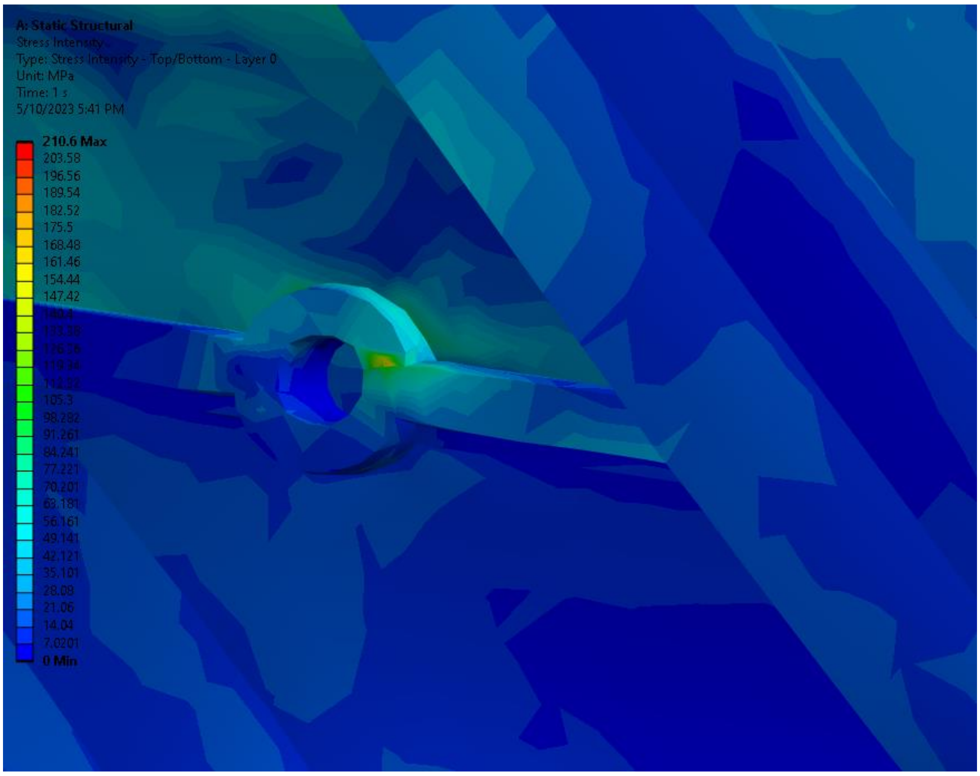

8. Validation: Loading conditions for 3.5 N, 8.5 N, 10.5 N, 12 N.

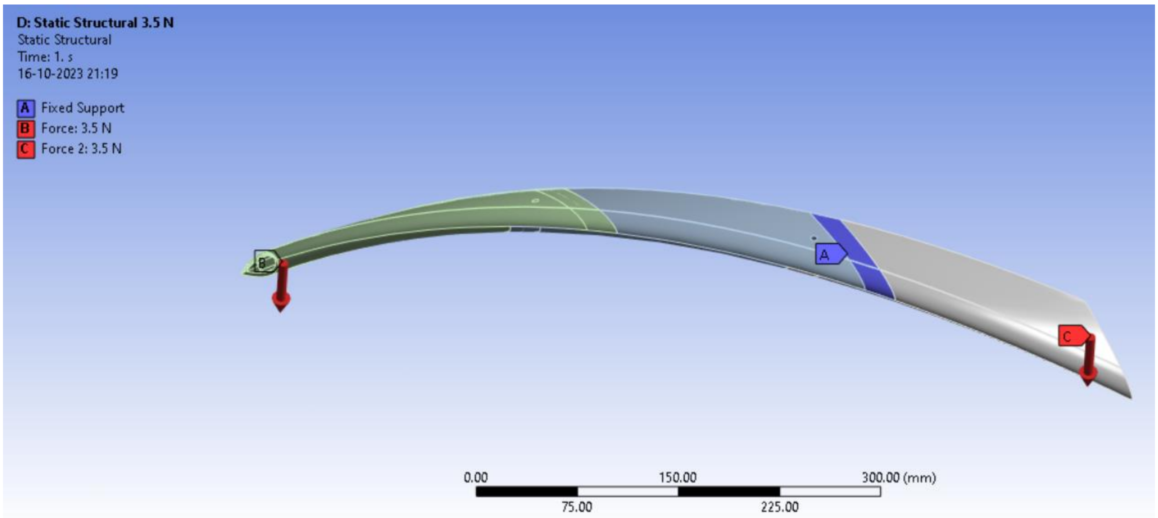

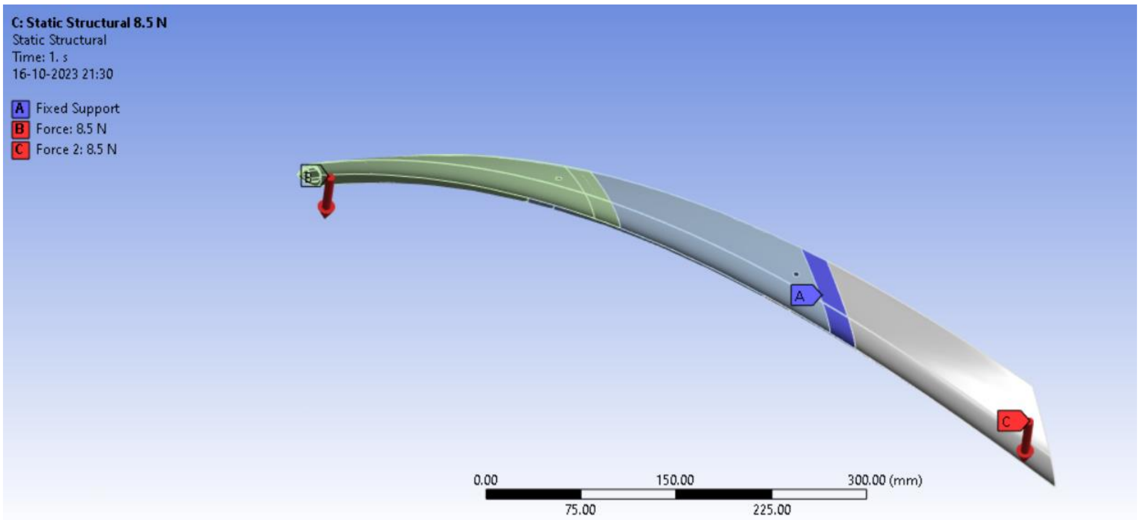

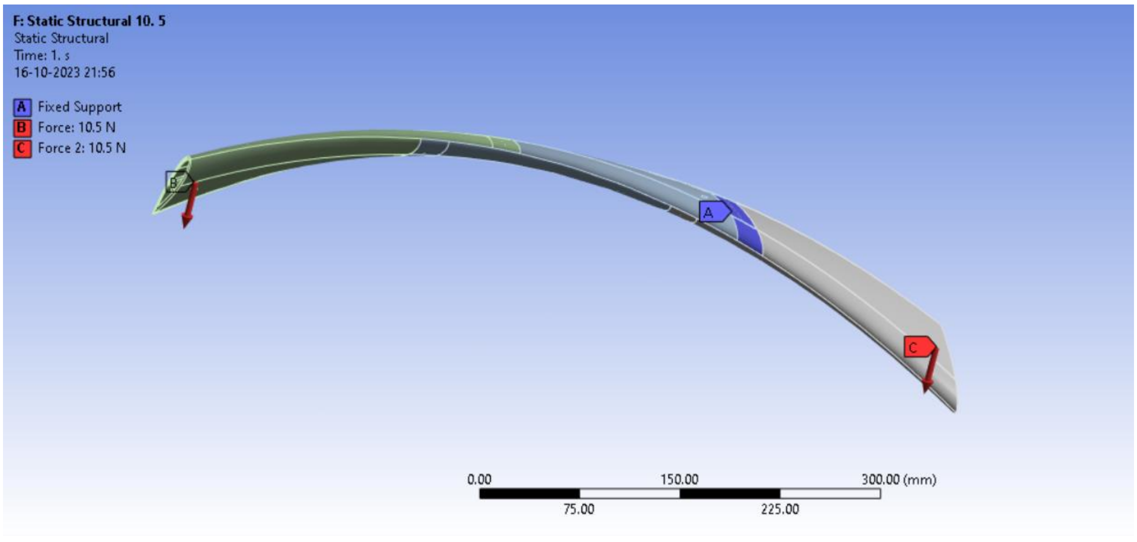

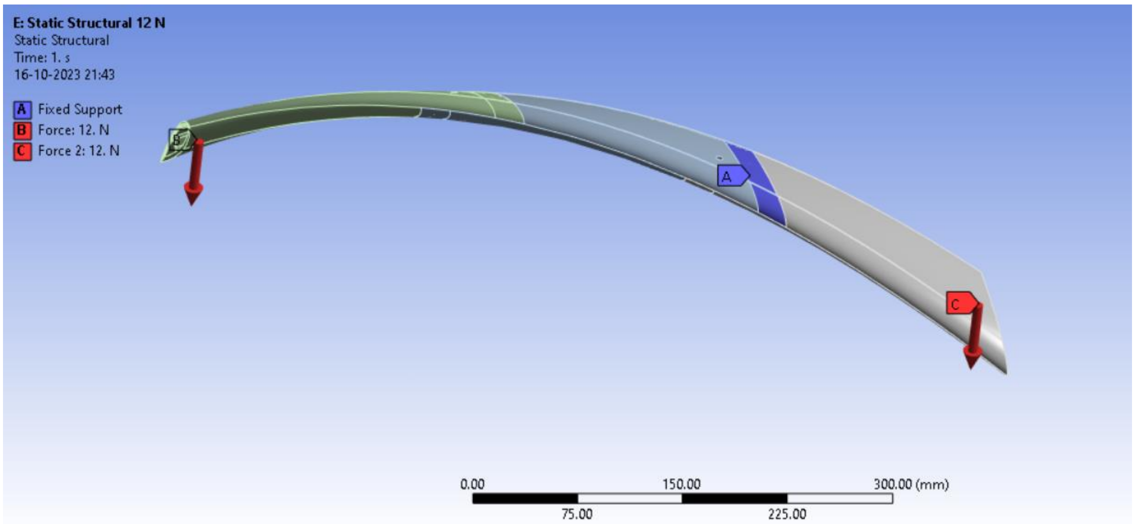

9. Validation: Results for 3.5 N, 8.5 N, 10.5 N, and 12 N Maximum shear stress, and stress Intensity.

i). 3.5 N

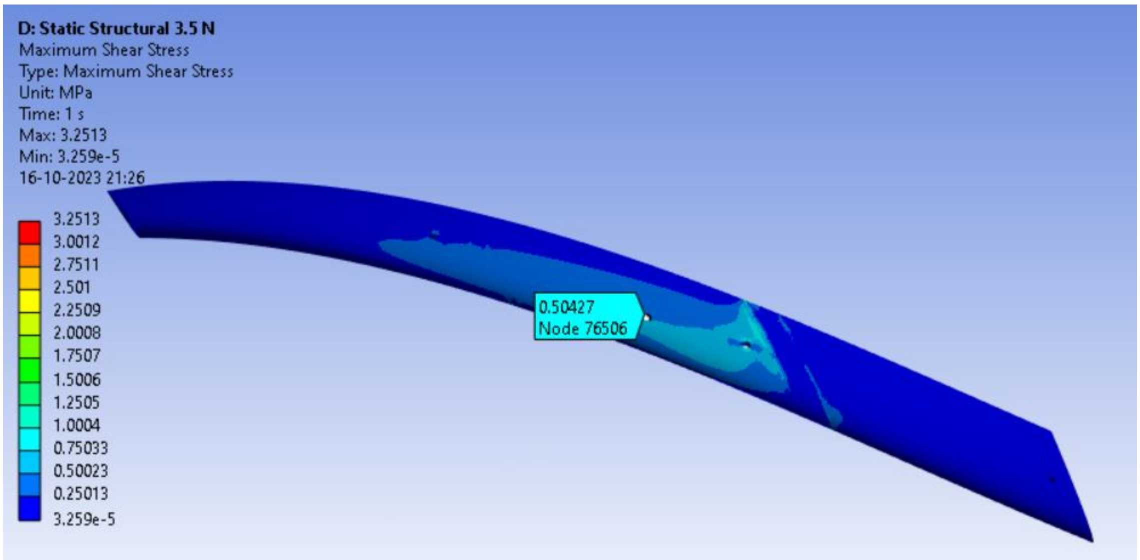
D: Static Structural 3.5 N
Maximum Shear Stress
Type: Maximum Shear Stress
Unit: MPa
Time: 1 s
Max: 3.2513
Min: 3.259e-5
16-10-2023 21:26
3.2513
3.0012
2.7511
2.501
2.2509
2.0008
1.7507
1.5006
1.2505
1.0004
0.75033
0.50023
0.25013
3.259e-5
0.50427
Node 76506

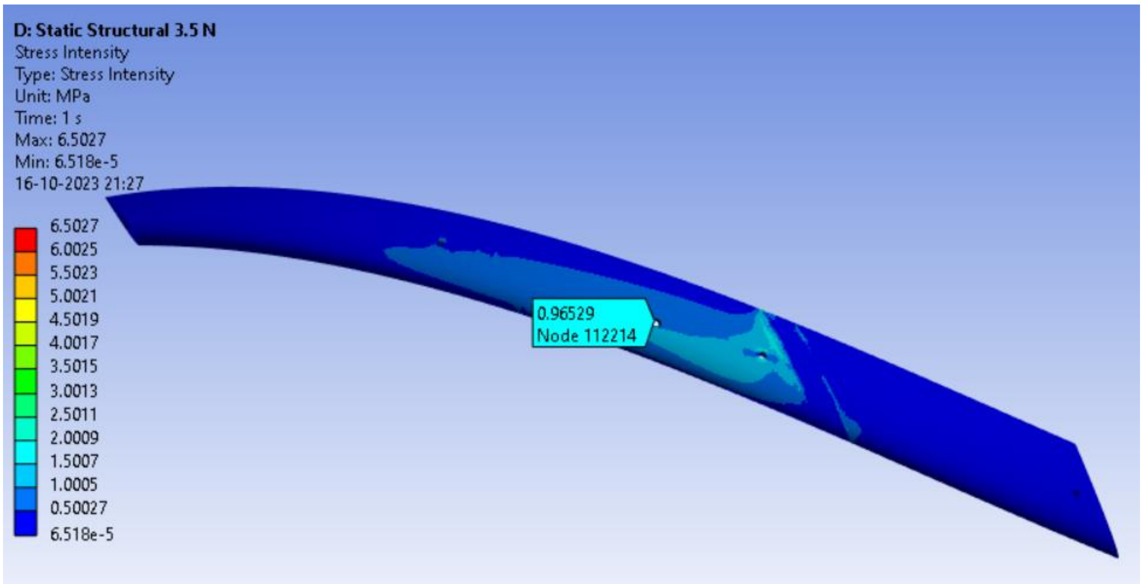
D: Static Structural 3.5 N
Stress Intensity
Type: Stress Intensity
Unit: MPa
Time: 1 s
Max: 6.5027
Min: 6.518e-5
16-10-2023 21:27
6.5027
6.0025
5.5023
5.0021
4.5019
4.0017
3.5015
3.0013
2.5011
2.0009
1.5007
1.0005
0.50027
6.518e-5
0.96529
Node 112214

ii). 8.5 N

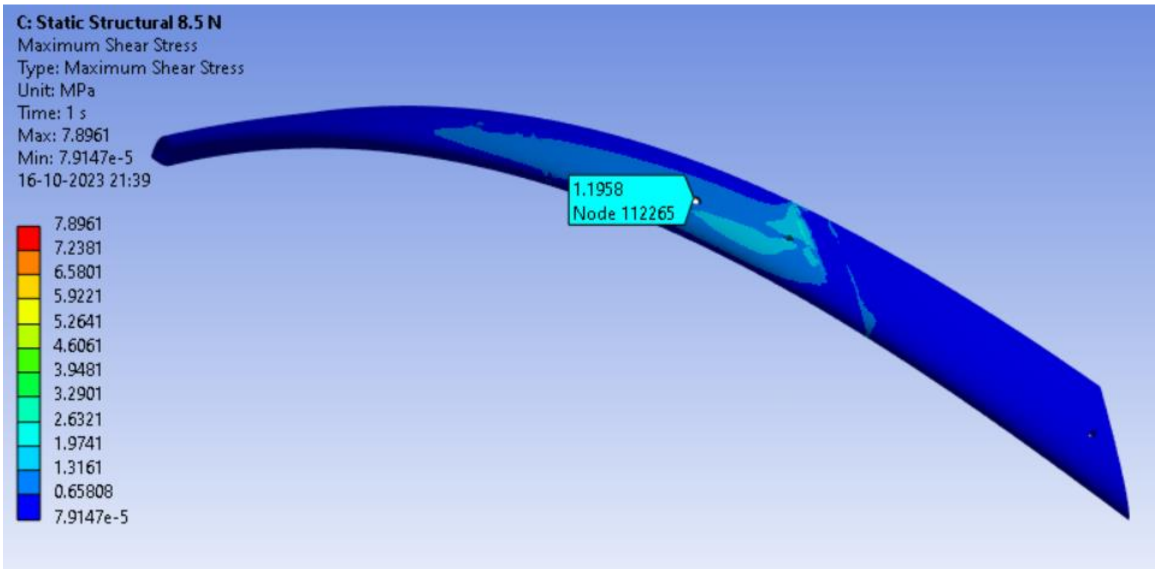
C: Static Structural 8.5 N
Maximum Shear Stress
Type: Maximum Shear Stress
Unit: MPa
Time: 1 s
Max: 7.8961
Min: 7.9147e-5
16-10-2023 21:39
7.8961
7.2381
6.5801
5.9221
5.2641
4.6061
3.9481
3.2901
2.6321
1.9741
1.3161
0.65808
7.9147e-5
1.1958
Node 112265

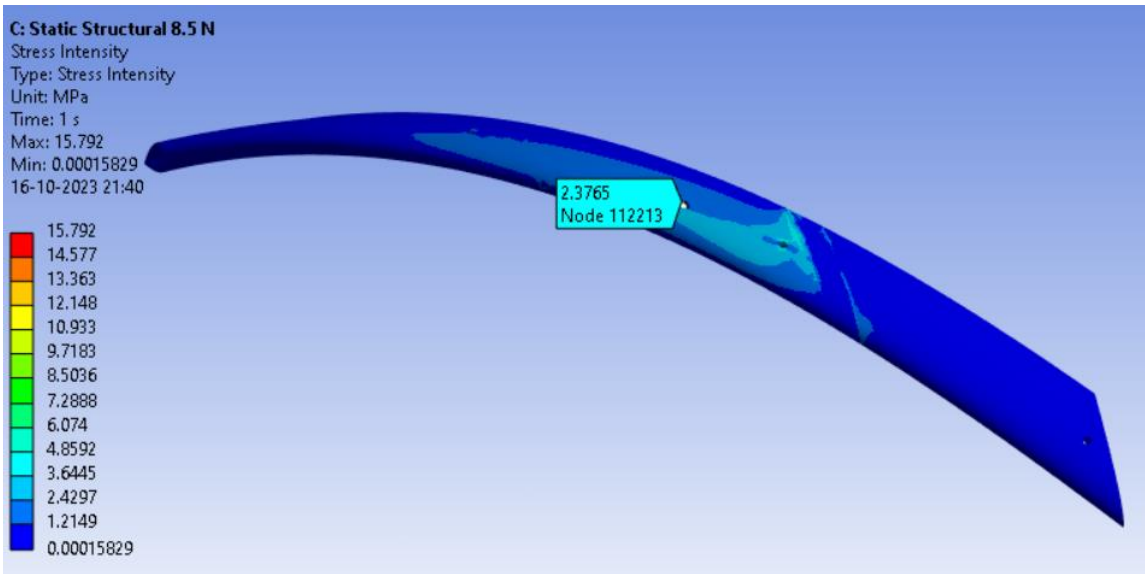
C: Static Structural 8.5 N
Stress Intensity
Type: Stress Intensity
Unit: MPa
Time: 1 s
Max: 15.792
Min: 0.00015829
16-10-2023 21:40
15.792
14.577
13.363
12.148
10.933
9.7183
8.5036
7.2888
6.074
4.8592
3.6445
2.4297
1.2149
0.00015829
2.3765
Node 112213

iii). 10.5 N

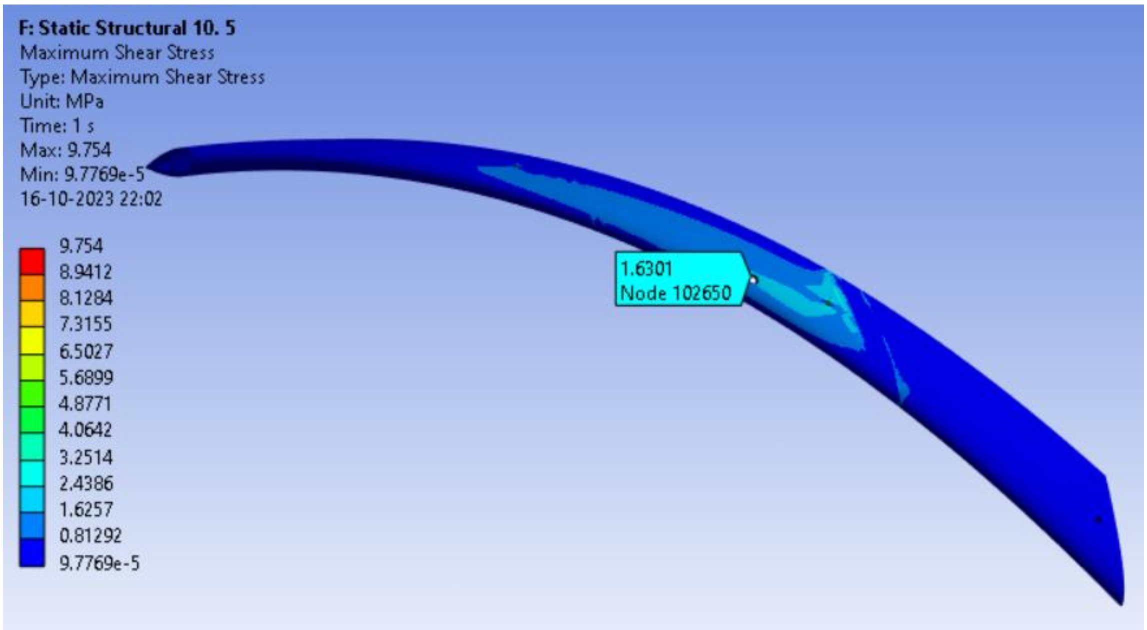
F: Static Structural 10. 5
Maximum Shear Stress
Type: Maximum Shear Stress
Unit: MPa
Time: 1 s
Max: 9.754
Min: 9.7769e-5
16-10-2023 22:02
9.754
8.9412
8.1284
7.3155
6.5027
5.6899
4.8771
4.0642
3.2514
2.4386
1.6257
0.81292
9.7769e-5
1.6301
Node 102650

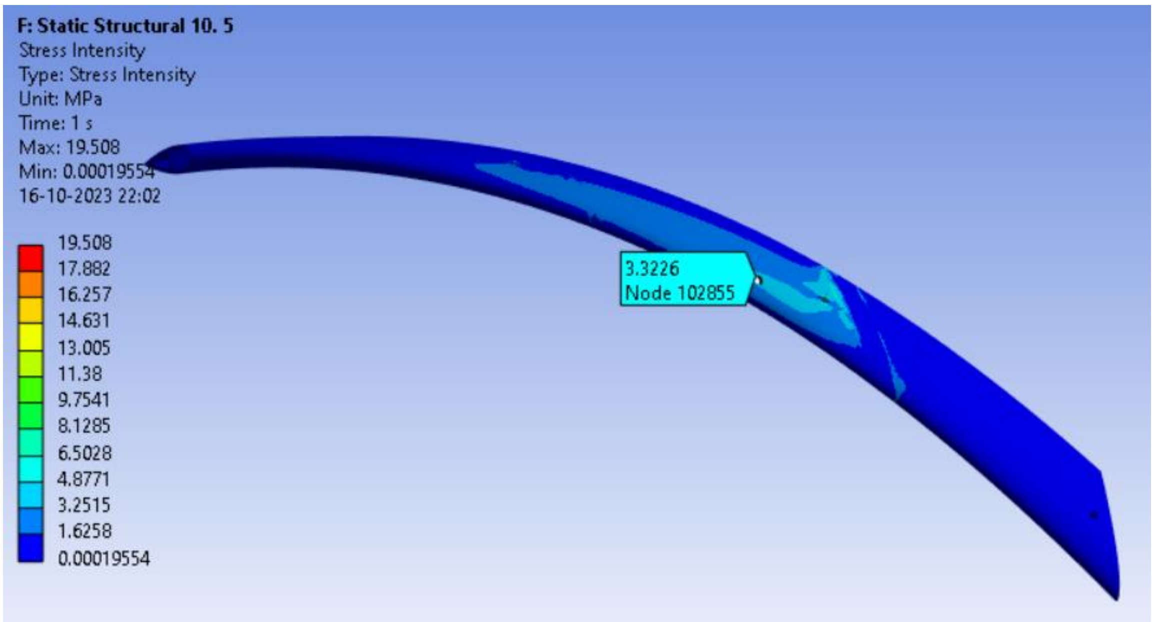
F: Static Structural 10. 5
Stress Intensity
Type: Stress Intensity
Unit: MPa
Time: 1 s
Max: 19.508
Min: 0.00019554
16-10-2023 22:02
19.508
17.882
16.257
14.631
13.005
11.38
9.7541
8.1285
6.5028
4.8771
3.2515
1.6258
0.00019554
3.3226
Node 102855

iv). 12 N

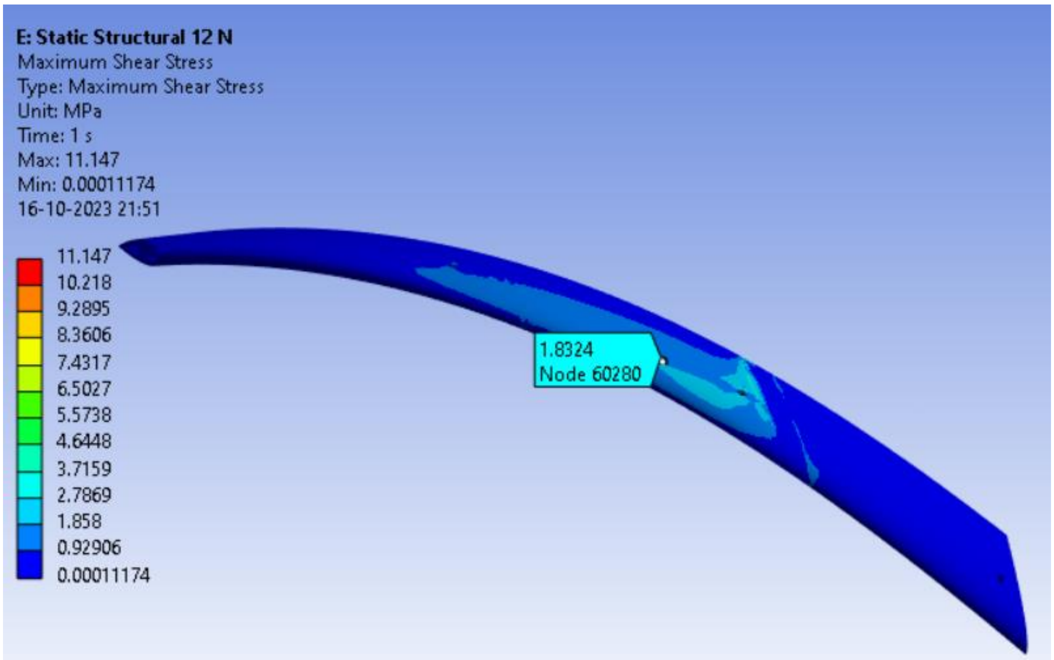
E: Static Structural 12 N
Maximum Shear Stress
Type: Maximum Shear Stress
Unit: MPa
Time: 1 s
Max: 11.147
Min: 0.00011174
16-10-2023 21:51
11.147
10.218
9.2895
8.3606
7.4317
6.5027
5.5738
4.6448
3.7159
2.7869
1.858
0.92906
0.00011174
1.8324
Node 60280

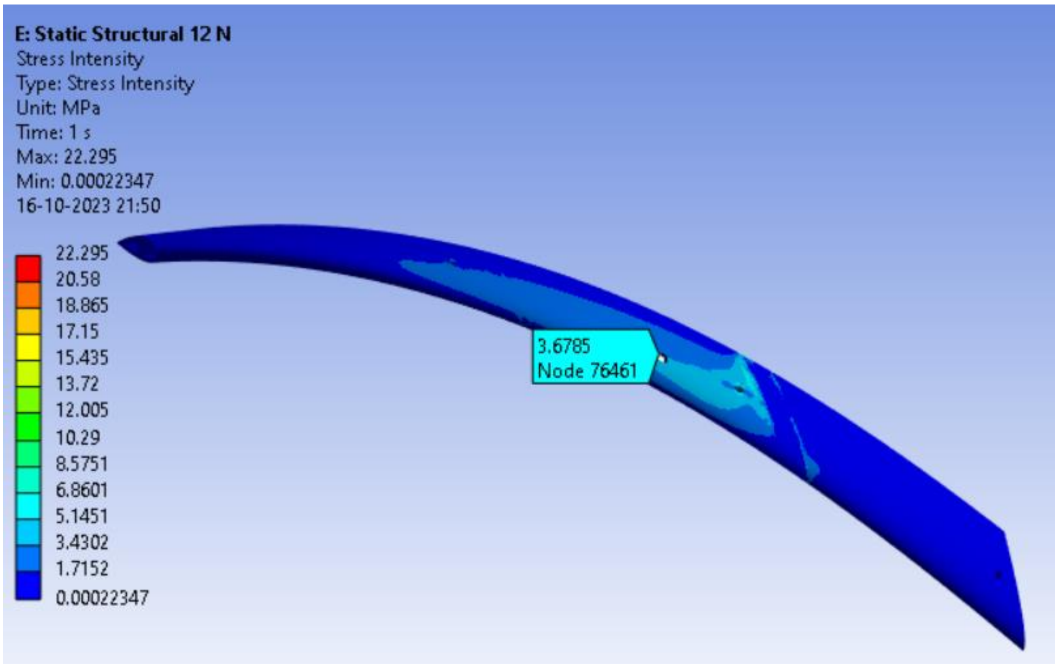
E: Static Structural 12 N
Stress Intensity
Type: Stress Intensity
Unit: MPa
Time: 1 s
Max: 22.295
Min: 0.00022347
16-10-2023 21:50
22.295
20.58
18.865
17.15
15.435
13.72
12.005
10.29
8.5751
6.8601
5.1451
3.4302
1.7152
0.00022347
3.6785
Node 76461